SC-R-68-1692
January 1968

Technical Report

MASTER

SCATTERING FROM IMPERFECTLY CONDUCTING SPHERES: NUMERICAL RESULTS

Charles W. Harrison, Jr., 1425
Margaret K. Houston, 1425
Sandia Laboratory, Albuquerque

SANDIA LABORATORIES

OPERATED FOR THE U. S. ATOMIC ENERGY COMMISSION BY SANDIA CORPORATION | ALBUQUERQUE, NEW MEXICO; LIVERMORE, CALIFORNIA

Issued by Sandia Corporation,
a prime contractor to the
United States Atomic Energy Commission

SC-R-68-1692

SCATTERING FROM IMPERFECTLY CONDUCTING SPHERES: NUMERICAL RESULTS*

Charles W. Harrison, Jr., 1425
Margaret K. Houston, 1425
Sandia Laboratory, Albuquerque

January 1968

ABSTRACT

Numerical results are presented based on a rigorous theory of scattering from imperfectly conducting spheres having positive and negative dielectric constants.

*This work was supported by the U.S. Atomic Energy Commission.

SUMMARY

Numerical data in the form of tables and graphs are presented for the back and forward scattering cross sections of imperfectly conducting homogeneous solid spheres. The spheres vary in electrical size over the range $0.001257 \leq k_o a \leq 50\pi$. Here k_o is the free space wave number and a is the radius of the sphere. However, the majority of the graphs were prepared for the cases $k_o a = \pi/2$ and π.

The relative dielectric constant ϵ_r and conductivity σ lie in the ranges $10^{-3} \leq \epsilon_r \leq 10^3$ and $10^{-7} \leq \sigma \leq 10^7$.

When $\sigma >> \omega\epsilon_o\epsilon_r$ it is shown that the back and forward scattering cross sections of the obstacle are essentially independent of ϵ and very insensitive to changes in σ; for practical purposes the body behaves as though it were perfectly conducting. This phenomenon also occurs for certain negative values of ϵ_r provided σ is not too large. Since there are large regions in which the scattering cross sections are very insensitive to both σ and ϵ, the writers concur with a comment made by Wyatt (1965) that "attempts to deduce the composition of large ionized volumes from radar measurements are of dubious practical utility, and indeed may be almost useless."[1]

The problem of radar return from a dust cloud is considered. It is shown that if $\epsilon_r \leq 30$, $\sigma \leq 3 \times 10^{-2}$ mhos/m and $a \leq 0.01$ m the scattering particle behaves as though it were a pure dielectric.

The forward scattering cross section of a sphere increases with increasing $k_o a$ when $\sigma >> \omega|\epsilon|$. No geometrical resonances are apparent.

TABLE OF CONTENTS

	Page
SUMMARY	3
Introduction	7
Discussion of Tables for the Back and Forward Scattering Cross Sections of Imperfectly Conducting Homogeneous Solid Spheres	9
On the Radar Cross Section of Small Earth Particles	12
Some Specific Comments on Scattering from Homogeneous Plasma Spheres Having Negative Dielectric Constants	15
Discussion of Curves for the Back and Forward Scattering Cross Sections of Imperfectly Conducting Homogeneous Solid Spheres	18
Conclusions	19
REFERENCES	20

LIST OF TABLES

Table		
I.	Imperfectly Conducting Homogeneous Sphere (Backward Scatter)	10
II.	Imperfectly Conducting Homogeneous Sphere (Backward Scatter)	11
III.	Imperfectly Conducting Homogeneous Sphere (Forward Scatter)	13
IV.	Imperfectly Conducting Homogeneous Sphere (Forward Scatter)	14
V.	Imperfectly Conducting Homogeneous Sphere (Backward Scatter)	16

LIST OF ILLUSTRATIONS

Figure		Page
1.	Backscattering Cross Section of a Perfectly Conducting Sphere	21
2.	Backscattering Cross Section of a Collisionless Plasma	22
3.	Backscattering Cross Section of a Sphere when $\sigma \gg \omega\|\epsilon\|$	23
4.	The Dependence of the Backscattering Cross Section of a Sphere on Conductivity for Fixed $k_o a$	24
5.	Like Figure 4, but for a Different Frequency	25
6.	Like Figure 4, but for a Different Frequency	26
7.	Like Figure 6, but for Negative Dielectric Constants	27
8.	Like Figure 6, but for a Different $k_o a$	28
9.	Like Figure 8, Except for Negative Dielectric Constants	29
10.	Like Figure 4, Except that Forward Scatter Cross-Section Data is Presented	30
11.	Like Figure 10, but for a Different Frequency	31
12.	Like Figure 10, Except for a Different Frequency	32
13.	Like Figure 12, Except for Negative Dielectric Constants	33
14.	Like Figure 12, Except for a Different $k_o a$	34
15.	Like Figure 14, Except for Negative Dielectric Constants	35
16.	Forward Scattering Cross Section of a Highly Conducting Sphere	36
17.	The Dependence of the Backscattering Cross Section of a Sphere on Relative Dielectric Constant for Fixed Conductivity	37
18.	Like Figure 17, but for a Different Value of Conductivity	38
19.	Like Figure 17, Except that Forward Scatter Cross-Section Data is Presented	39
20.	Like Figure 19, but for a Different Value of Conductivity	40

SCATTERING FROM IMPERFECTLY CONDUCTING SPHERES: NUMERICAL RESULTS

Introduction

It is shown in the companion paper by Harrison[2] that the back scattered and forward scattered electric fields from a homogeneous solid sphere may be written

$$E_r = -j\hat{x}\,\frac{E_o}{2}\,\frac{e^{-jk_oR}}{k_oR}\sum_{n=1}^{\infty}(-1)^n(2n+1)\left(a_n^r - b_n^r\right), \tag{1}$$

and

$$E_r = -j\hat{x}\,\frac{E_o}{2}\,\frac{e^{-jk_oR}}{k_oR}\sum_{n=1}^{\infty}(2n+1)\left(a_n^r + b_n^r\right), \tag{2}$$

respectively. Here E_o is the amplitude of the incident field, k_o is the free space wave number, and R is the distance from the center of the sphere to the point the scattered field E_r is to be determined. For an assumed (but suppressed) time dependence exp $(j\omega t)$ the constants a_n^r and b_n^r have the values

$$a_n^r = - \frac{j_n(k_o a)\left[k_1 a j_n(k_1 a)\right]' - j_n(k_1 a)\left[k_o a j_n(k_o a)\right]'}{h_n^{(2)}(k_o a)\left[k_1 a j_n(k_1 a)\right]' - j_n(k_1 a)\left[k_o a h_n^{(2)}(k_o a)\right]'} , \quad (3)$$

and

$$b_n^r = - \frac{k_1^2 j_n(k_1 a)\left[k_o a j_n(k_o a)\right]' - k_o^2 j_n(k_o a)\left[k_1 a j_n(k_1 a)\right]'}{k_1^2 j_n(k_1 a)\left[k_o a h_n^{(2)}(k_o a)\right]' - k_o^2 h_n^{(2)}(k_o a)\left[k_1 a j_n(k_1 a)\right]'} , \quad (4)$$

where k_1 is the propagation constant of the sphere, and a is its radius. In writing Equations 3 and 4 it is assumed that the permeability of the sphere is the same as that of free space. With $\mu = \mu_o$ and $\epsilon < 0$,

$$k_1 = \beta - j\alpha = \sqrt{-\omega^2 \mu |\epsilon| - j\sigma\omega\mu} = k_o \sqrt{|\epsilon_r|}\,[g(p) - jf(p)] \; . \quad (5)$$

If $\epsilon > 0$,

$$k_1 = k_o \sqrt{\epsilon_r}\,[f(p) - jg(p)] \; . \quad (6)$$

In addition, if the inequality

$$p = \frac{\sigma}{\omega |\epsilon|} = \frac{\sigma}{\omega \epsilon_o |\epsilon_r|} >> 1 \quad (7)$$

is satisfied,

$$k_1 = \sqrt{\frac{\omega\mu\sigma}{2}}(1 - j) , \quad (8)$$

k_1 as given by Equation 8 is valid when $\epsilon = 0$. Also,

$$f(p) = \cosh\left(\frac{1}{2}\sinh^{-1} p\right) , \tag{9}$$

and

$$g(p) = \sinh\left(\frac{1}{2}\sinh^{-1} p\right) = p/2f(p) . \tag{10}$$

Evidently when $p \gg 1$, $f(p) \to g(p) \to \sqrt{\frac{p}{2}}$ and when $p \ll 1$, $f(p) \to 1$, $g(p) \to \frac{p}{2}$. Notice also that

$$\left[\rho z_n(\rho)\right]' = \left[z_{n-1}(\rho) - \frac{n}{\rho} z_n(\rho)\right]\rho . \tag{11}$$

The scattering cross section of an obstacle is given by the formula

$$\sigma_{\substack{s \\ f}} = \lim_{R \to \infty} 4\pi R^2 \left|\frac{E_r}{E_o}\right|^2 . \tag{12}$$

σ_s is the back-scattering cross section; σ_f is the forward-scattering cross section.

Discussion of Tables for the Back and Forward Scattering Cross Sections of Imperfectly Conducting Homogeneous Solid Spheres

Table I presents σ_s/λ_o^2 and $\sigma_s/\pi a^2$ as a function of σ for several frequencies when $k_o a = \pi/2$. For these data $\sigma \gg \omega|\epsilon|$ and $k = \sqrt{\frac{\omega\mu\sigma}{2}}(1 - j)$. Evidently the results are very insensitive to changes in σ. For all practical purposes the scattering obstacle behaves as though it were perfectly conducting and $\sigma_s/\pi a^2$ may be obtained for a particular value of $k_o a$ from Figure 1. Table II is similar to Table I except that several frequencies and values of $k_o a$ are used. It is

TABLE I

Imperfectly Conducting Homogeneous Sphere
(Backward Scatter)

$k_o a = \pi/2$, f = 8.78 MHz			$k_o a = \pi/2$, f = 50 MHz			$k_o a = \pi/2$, f = 10 MHz		
σ	σ_s/λ_o^2	$\sigma_s/\pi a^2$	σ	σ_s/λ_o^2	$\sigma_s/\pi a^2$	σ	σ_s/λ_o^2	$\sigma_s/\pi a^2$
10^{-1}	0.0914	0.4657	10^{0}	0.1013	0.5159	10^{-1}	0.0889	0.4527
10^{0}	0.1210	0.6163	10^{1}	0.1248	0.6355	10^{0}	0.1200	0.6111
10^{1}	0.1318	0.6711	10^{2}	0.1330	0.6775	10^{1}	0.1314	0.6693
10^{2}	0.1353	0.6891	10^{3}	0.1357	0.6912	10^{2}	0.1352	0.6886
10^{3}	0.1364	0.6949	10^{4}	0.1366	0.6956	10^{3}	0.1364	0.6947
10^{4}	0.1368	0.6968	10^{5}	0.1369	0.6970	10^{4}	0.1368	0.6967
10^{5}	0.1369	0.6973	10^{6}	0.1369	0.6974	10^{5}	0.1369	0.6973
10^{6}	0.1370	0.6975	10^{7}	0.1370	0.6976	10^{6}	0.1370	0.6975
10^{7}	0.1370	0.6976				10^{7}	0.1370	0.6976

TABLE II

Imperfectly Conducting Homogeneous Sphere
(Backward Scatter)

$k_o a = 0.5$, f = 2.795 MHz

σ	σ_s/λ_o^2	$\sigma_s/\pi a^2$
10^{-1}	0.0099	0.4952
10^0	0.0103	0.5185
10^1	0.0105	0.5260
10^2	0.0105	0.5285
10^3	0.0105	0.5292
10^4	0.0105	0.5295
10^5	0.0105	0.5295
10^6	0.0105	0.5296
10^7	0.0105	0.5297

$k_o a = 3.0$, f = 2.795 MHz

σ	σ_s/λ_o^2	$\sigma_s/\pi a^2$
10^{-1}	0.3273	0.4570
10^0	0.3565	0.4978
10^1	0.3676	0.5132
10^2	0.3712	0.5184
10^3	0.3724	0.5200
10^4	0.3728	0.5205
10^5	0.3729	0.5207
10^6	0.3730	0.5207
10^7	0.3730	0.5208

$k_o a = 5\pi$, f = 200 MHz

σ	σ_s/λ_o^2	$\sigma_s/\pi a^2$
10^1	18.87	0.9612
10^2	20.31	1.034
10^3	20.75	1.057
10^4	20.89	1.064
10^5	20.94	1.066
10^6	20.95	1.067
10^7	20.96	1.067

$k_o a = 1.0$, f = 2.795 MHz

σ	σ_s/λ_o^2	$\sigma_s/\pi a^2$
10^{-1}	0.2752	3.458
10^0	0.2850	3.582
10^1	0.2881	3.620
10^2	0.2890	3.632
10^3	0.2893	3.636
10^4	0.2894	3.637
10^5	0.2895	3.637
10^6	0.2895	3.638
10^7	0.2895	3.638

$k_o a = \pi$, f = 200 MHz

σ	σ_s/λ_o^2	$\sigma_s/\pi a^2$
10	0.5759	0.7333
10^2	0.5875	0.7480
10^3	0.5919	0.7536
10^4	0.5934	0.7555
10^5	0.5939	0.7561
10^6	0.5940	0.7563
10^7	0.5941	0.7564

$k_o a = 50\pi$, f = 200 MHz

σ	σ_s/λ_o^2	$\sigma_s/\pi a^2$
10^1	1786.5	0.9100
10^2	1905.5	0.9705
10^3	1944.9	0.9905
10^4	1957.5	0.9970
10^5	1961.5	0.9990
10^6	1962.8	0.9997
10^7	1963.2	0.9999

important to note that $k_o a \geq 5\pi$, $\sigma_s/\pi a^2 \to 1.0$. This is in evidence both from Figure 1 and Table II. Tables III and IV complement Tables I and II, respectively, except that σ_f/λ_o^2 and $\sigma_f/\pi a^2$ as a function of σ are presented. As long as $\sigma \gg \omega|\epsilon|$ one must expect the forward scattering cross section--and more generally the bistatic scattering cross section--to be essentially independent of ϵ and very insensitive to changes in σ.

On the Radar Cross Section of Small Earth Particles

The radar cross section of homogeneous spheres of several small radii consisting of dry earth ($\epsilon_r = 7$, $\sigma = 10^{-3}$ mhos/m), damp earth ($\epsilon_r = 15$, $\sigma = 12 \times 10^{-3}$ mhos/m), and wet earth ($\epsilon_r = 30$, $\sigma = 30 \times 10^{-3}$ mhos/m) was determined so that the radar return from a dust cloud could be calculated. These data are presented in Table V. (It should be mentioned that in all of the computations reported in this paper the computer program was not modified regardless of sphere size.) The average cross section of the dust cloud is

$$\bar{\sigma} = \sum_{i=1}^{n} \sigma_i .$$

If the particles are the same size and possess the same electrical properties, evidently $\bar{\sigma} = n\sigma_s$, where n is the number of particles. In these relations the interaction of the spheres upon one another is neglected. It should be noticed that when the dust particles are small, for example, a = 0.01 m, $\sigma_s/\pi a^2$ is independent of σ to the accuracy reported in the table. In other words, the dust cloud is just another rain drop cloud of changed dielectric constant. However, for this size particle when $f = 2 \times 10^9$ Hz and $\sigma > 0.5$ mhos/m, the conductivity becomes important. Specifically, when $\sigma = 1$ mho/m, $\sigma_s/\pi a^2 = 0.0907$, 0.0853 and 0.0662 for $\epsilon_r = 7.0$, 15.0, and 30.0, respectively. For the circumstances described above, $\sigma_s/\pi a^2 = 0.2605$ whenever $\sigma \gg \omega|\epsilon|$.

TABLE III

Imperfectly Conducting Homogeneous Sphere
(Forward Scatter)

$k_o a = \pi/2$, f = 8.78 MHz			$k_o a = \pi/2$, f = 50 MHz			$k_o a = \pi/2$, f = 10 MHz		
σ	σ_f/λ_o^2	$\sigma_f/\pi a^2$	σ	σ_f/λ_o^2	$\sigma_f/\pi a^2$	σ	σ_f/λ_o^2	$\sigma_f/\pi a^2$
10^{-1}	0.7752	3.948	10^{0}	0.7327	3.732	10^{-1}	0.7867	4.007
10^{0}	0.6565	3.343	10^{1}	0.6430	3.275	10^{0}	0.6602	3.362
10^{1}	0.6189	3.152	10^{2}	0.6147	3.131	10^{1}	0.6201	3.158
10^{2}	0.6071	3.092	10^{3}	0.6058	3.085	10^{2}	0.6075	3.094
10^{3}	0.6034	3.073	10^{4}	0.6029	3.071	10^{3}	0.6035	3.073
10^{4}	0.6022	3.067	10^{5}	0.6020	3.066	10^{4}	0.6022	3.067
10^{5}	0.6018	3.065	10^{6}	0.6018	3.065	10^{5}	0.6018	3.065
10^{6}	0.6017	3.064	10^{7}	0.6017	3.064	10^{6}	0.6017	3.064
10^{7}	0.6016	3.064				10^{7}	0.6016	3.064

TABLE IV

Imperfectly Conducting Homogeneous Sphere
(Forward Scatter)

$k_o a = 0.5$, $f = 2.795$ MHz

σ	σ_f/λ_o^2	$\sigma_s/\pi a^2$
10^{-1}	2.750×10^{-3}	0.1383
10^{0}	2.211×10^{-3}	0.1111
10^{1}	2.053×10^{-3}	0.1032
10^{2}	2.005×10^{-3}	0.1008
10^{3}	1.990×10^{-3}	0.1000
10^{4}	1.985×10^{-3}	0.0998
10^{5}	1.983×10^{-3}	0.0997
10^{6}	1.983×10^{-3}	0.0997
10^{7}	1.983×10^{-3}	0.0997

$k_o a = 3.0$, $f = 2.795$ MHz

σ	σ_f/λ_o^2	$\sigma_f/\pi a^2$
10^{-1}	8.763	12.24
10^{0}	8.060	11.25
10^{1}	7.836	10.94
10^{2}	7.765	10.84
10^{3}	7.743	10.81
10^{4}	7.736	10.80
10^{5}	7.734	10.80
10^{6}	7.733	10.80
10^{7}	7.733	10.80

$k_o a = 5\pi$, $f = 200$ MHz

σ	σ_f/λ_o^2	$\sigma_f/\pi a^2$
10^{1}	5.356×10^{3}	2.728×10^{2}
10^{2}	5.145×10^{3}	2.620×10^{2}
10^{3}	5.077×10^{3}	2.586×10^{2}
10^{4}	5.056×10^{3}	2.575×10^{2}
10^{5}	5.050×10^{3}	2.572×10^{2}
10^{6}	5.047×10^{3}	2.571×10^{2}
10^{7}	5.047×10^{3}	2.570×10^{2}

$k_o a = 1.0$, $f = 2.795$ MHz

σ	σ_f/λ_o^2	$\sigma_f/\pi a^2$
10^{-1}	0.1619	2.034
10^{0}	0.1430	1.797
10^{1}	0.1371	1.722
10^{2}	0.1352	1.698
10^{3}	0.1346	1.691
10^{4}	0.1344	1.689
10^{5}	0.1343	1.688
10^{6}	0.1343	1.688
10^{7}	0.1343	1.688

$k_o a = \pi$, $f = 200$ MHz

σ	σ_f/λ_o^2	$\sigma_f/\pi a^2$
10^{1}	10.25	13.05
10^{2}	9.565	12.18
10^{3}	9.348	11.90
10^{4}	9.280	11.82
10^{5}	9.258	11.79
10^{6}	9.251	11.78
10^{7}	9.249	11.78

$k_o a = 50\pi$, $f = 200$ MHz

σ	σ_f/λ_o^2	$\sigma_f/\pi a^2$
10^{1}	5.005×10^{7}	2.549×10^{4}
10^{2}	4.915×10^{7}	2.503×10^{4}
10^{3}	4.886×10^{7}	2.488×10^{4}
10^{4}	4.876×10^{7}	2.484×10^{4}
10^{5}	4.873×10^{7}	2.482×10^{4}
10^{6}	4.873×10^{7}	2.482×10^{4}
10^{7}	4.872×10^{7}	2.481×10^{4}

It is of interest to compare these results with those obtained from an expression derived by Siegert (1947).[3] His formula for a dielectric sphere (Rayleigh scattering region, $k_o a < 2\pi \times 10^{-1}$) is

$$\sigma_s/\pi a^2 = 4(k_o a)^4\left(\frac{\epsilon_r - 1}{\epsilon_r + 2}\right)^2 .$$

From this one obtains $\sigma_s/\pi a^2 = 5.4742 \times 10^{-2}$, 8.3534×10^{-2}, 1.0116×10^{-1}, and 1.1443×10^{-1} for ϵ_r = 7.0, 15.0, 30.0, and 81.0, respectively. Comparing these results with those presented in Table V for a = 0.01 m shows that agreement is not good when ϵ_r is large.

It is worthy of mention that Table V shows, for example, that when $\sigma = 0$ (a condition that is not physically realizable) and a = 0.035 m, $\sigma_s/\pi a^2$ is much larger for $\epsilon_r = 15$ than for $\epsilon_r = 81$. This result is not surprising when it is remembered that multiple reflections within the dielectric sphere may give rise to a larger bistatic cross section thanmono-static cross section.

Some Specific Comments on Scattering from Homogeneous Plasma Spheres Having Negative Dielectric Constants

Figure 2 was reproduced from a paper by Wyatt (1965)[1] except that N is measured in electrons/cu m. This curve was computed for a collisionless homogeneous plasma sphere when $k_o a = 40.0$ and f = 1.27236 kMHz. Under these conditions the relative dielectric constant is given by $\epsilon_r = 1 - 0.49796 \times 10^{-16}$ N. Of great significance is the fact that in the region $8 \times 10^{16} < N < 2 \times 10^{18}$ corresponding to $-2.9837 > \epsilon_r > -98.592$ sharp oscillations in the radar cross section occur. In the regions $-2.9837 < \epsilon_r < 0$ and $\epsilon_r < -98.592$ the sphere behaves as though it were perfectly conducting. From Figures 1 and 2 for $k_o a = 40$, $\sigma_s/\pi a^2 \simeq 1.0$. This striking effect has been explained by Wyatt (1966)[4] in terms of destructive and constructive interference of surface waves

TABLE V

Imperfectly Conducting Homogeneous Sphere (Backward Scatter)

$a = 0.035$ m; $k_o a = 1.466$; $f = 2 \times 10^9$ Hz

ϵ_r	σ	σ_s/λ_o^2	$\sigma_s/\pi a^2$
7	10^{-3}	0.4770	2.783
7	0.0	0.4798	2.805
15	1.2×10^{-2}	0.7857	4.593
15	0.0	2.349	16.656
30	3.0×10^{-2}	0.0122	0.0711
30	0.0	0.0219	0.1279
81	0.0	0.3448	2.016

$a = 0.00003$; $k_o a = 0.001257$; $f = 2 \times 10^9$ Hz

ϵ_r	σ	σ_s/λ_o^2	$\sigma_s/\pi a^2$
7	10^{-3}	5.574×10^{-19}	4.436×10^{-12}
7	0.0	5.574×10^{-19}	4.436×10^{-12}
15	1.2×10^{-2}	8.503×10^{-19}	6.767×10^{-12}
15	0.0	8.502×10^{-19}	6.766×10^{-12}
30	3.0×10^{-2}	1.030×10^{-18}	8.193×10^{-12}
30	0.0	1.030×10^{-18}	8.193×10^{-12}
81	0.0	1.164×10^{-18}	9.266×10^{-12}

$a = 0.001$; $k_o a = 0.0419$; $f = 2 \times 10^9$ Hz

ϵ_r	σ	σ_s/λ_o^2	$\sigma_s/\pi a^2$
7	10^{-3}	7.646×10^{-10}	5.476×10^{-6}
7	0.0	7.646×10^{-10}	5.476×10^{-6}
15	1.2×10^{-2}	1.166×10^{-9}	8.349×10^{-6}
15	0.0	1.166×10^{-9}	8.349×10^{-6}
30	3.0×10^{-2}	1.409×10^{-9}	1.009×10^{-5}
30	0.0	1.409×10^{-9}	1.009×10^{-5}
81	0.0	1.585×10^{-9}	1.135×10^{-5}

$a = 0.003$; $k_o a = 0.1257$; $f = 2 \times 10^9$ Hz

ϵ_r	σ	σ_s/λ_o^2	$\sigma_s/\pi a^2$
7	10^{-3}	5.564×10^{-7}	4.428×10^{-4}
7	0.0	5.564×10^{-7}	4.428×10^{-4}
15	1.2×10^{-2}	8.448×10^{-7}	6.723×10^{-4}
15	0.0	8.448×10^{-7}	6.723×10^{-4}
30	3.0×10^{-2}	1.008×10^{-6}	8.021×10^{-4}
30	0.0	1.008×10^{-6}	8.021×10^{-4}
81	0.0	1.069×10^{-6}	8.509×10^{-4}

$a = 0.01$ m; $k_o a = 0.4189$; $f = 2 \times 10^9$ Hz

ϵ_r	σ	σ_s/λ_o^2	$\sigma_s/\pi a^2$
7	10^{-3}	7.436×10^{-4}	5.325×10^{-2}
7	0.0	7.436×10^{-4}	5.325×10^{-2}
15	1.2×10^{-2}	1.035×10^{-3}	7.408×10^{-2}
15	0.0	1.035×10^{-3}	7.410×10^{-2}
30	3.0×10^{-2}	7.059×10^{-4}	5.055×10^{-2}
30	0.0	7.062×10^{-4}	5.058×10^{-2}
81	0.0	6.555×10^{-3}	4.694×10^{-1}

$a = 0.0001$; $k_o a = 0.0042$; $f = 2 \times 10^9$ Hz

ϵ_r	σ	σ_s/λ_o^2	$\sigma_s/\pi a^2$
7	10^{-3}	7.647×10^{-16}	5.477×10^{-10}
7	0.0	7.647×10^{-16}	5.477×10^{-10}
15	1.2×10^{-2}	1.167×10^{-15}	8.355×10^{-10}
15	0.0	1.167×10^{-15}	8.355×10^{-10}
30	3.0×10^{-2}	1.412×10^{-15}	1.012×10^{-9}
30	0.0	1.412×10^{-15}	1.012×10^{-9}
81	0.0	1.597×10^{-15}	1.144×10^{-9}

$a = 0.0003$; $k_o a = 0.01257$; $f = 2 \times 10^9$ Hz

ϵ_r	σ	σ_s/λ_o^2	$\sigma_s/\pi a^2$
7	10^{-3}	5.574×10^{-13}	4.436×10^{-8}
7	0.0	5.574×10^{-13}	4.436×10^{-8}
15	1.2×10^{-2}	8.502×10^{-13}	6.766×10^{-8}
15	0.0	8.502×10^{-13}	6.766×10^{-8}
30	3.0×10^{-2}	1.029×10^{-12}	8.191×10^{-8}
30	0.0	1.029×10^{-12}	8.191×10^{-8}
81	0.0	1.164×10^{-12}	9.260×10^{-8}

Dry Earth: $\epsilon_r = 7$, $\sigma = 10^{-3}$ mhos/m

Damp Earth: $\epsilon_r = 15$, $\sigma = 12 \times 10^{-3}$ mhos/m

Wet Earth: $\epsilon_r = 30$, $\sigma = 30 \times 10^{-3}$ mhos/m with the backscattered ray. He furnishes a simple method for calculating ϵ_r in the region where the anomalous oscillations occur. The fact that this phenomenon exists was verified by the writers, using the CDC-6600 computer program on which all numerical data presented in this paper is based. For $k_o a = 40$, f = 1.27236 kMHz, and $\sigma = 10^{-10}$, the following results were obtained:

ϵ_r	$\sigma_s/\pi a^2$
0.95	4.409×10^{-4}
-1.00	1.001
-3.79	0.6604
-10.10	0.4107
-15.44	2.572

A calculation was also made to determine if oscillations are generated by changing σ on the peak values of $\sigma_s/\pi a^2$ predicted by Wyatt (1965).[1] For example, if $\epsilon_r = -15.44$, then $\sigma_s/\pi a^2$ = 2.572, 2.572, 2.572, 2.571, 2.563, 2.481, 1.858, and 0.7813, as σ increases by decades from 10^{-7} through 10^0, respectively. Thus no oscillations are indicated in this range of σ. (Nine values of back scattering cross section were computed between each listing entered above.) In general, in making the calculations presented in this paper ϵ_r, $k_o a$ and f were fixed and the back or forward scatter cross sections determined for a mesh size in σ of one decade. Whether or not anomalous behavior in the results is possible for smaller incremental values in σ was not investigated either theoretically or by use of the computer. No investigation was made to insure that oscillations are absent when $\epsilon_r < -98.59$. From numerous curves presented subsequently in this paper it is evident that oscillations exist even when $\sigma \searrow 0$. Plots of $\sigma_s/\pi a^2$ against ϵ_r for fixed σ, f and $k_o a$ are oscillatory in character. This follows from the fact that for fixed f and $k_o a$ curves of $\sigma_s/\pi a^2$ against σ with ϵ_r as parameter are not in numerical sequence insofar as ϵ_r is concerned.

Discussion of Curves for the Back and Forward Scattering Cross Sections of Imperfectly Conducting Homogeneous Solid Spheres

In obtaining data for the preparation of the graphs, Figures 3-20, the writers wish to emphasize that an exhaustive search for anomalies in the back and forward scattering cross sections of an imperfectly conducting homogeneous sphere was not undertaken. In the case of each graph what the authors deemed to be a reasonable number of points were computed and plotted. For example, in the preparation of Figures 17-20 200 points equally spaced in ϵ_r were computed for each graph. So it is possible (but not likely) that some sharp oscillations in the cross sections were overlooked. Of course, the anomalies, if they exist, could be found for slightly lossy plasmas by the means suggested by Wyatt (1966).[4] One might expect such oscillations to be of decreasing amplitude as σ is increased.

Figures 3-20 are largely self-explanatory. In the interest of brevity only a few comments will be made relating to the graphs. Notice that Figures 10-15 for $\sigma_f/\pi a^2$ against $k_o a$ complement Figures 4-9 for $\sigma_s/\pi a^2$ against $k_o a$. Remember that scaling of these data is possible. When $\sigma \gg \omega|\epsilon|$ the sphere behaves as though it were perfectly conducting. This is shown by Figure 3 (complemented by Figure 1 as well as by Figures 4-9). This same phenomenon, to lesser degree, was observed by Taylor, et al (1967)[5] for the backscattering cross section of a resistive cylinder of finite length. Figure 16 is of special interest in that it shows that $\sigma_f/\pi a^2$ can be progressively increased with increasing $k_o a(\sigma \gg \omega|\epsilon|)$. This is in contrast to the limit of 1.0 approached by $\sigma_s/\pi a^2$ as $k_o a \rightarrow \infty$ (Figure 1). Comparing Figure 17 with Figure 18 and Figure 19 with Figure 20, it is evident that as σ is increased the amplitudes of the oscillations in $\sigma_s/\pi a^2$ and $\sigma_f/\pi a^2$ are decreased.

Conclusions

Assuming that $k_o a$ is constant, an examination of Equations 3 and 4 reveals that if one can prove $k_1 a$ relatively constant with changes in ϵ_r, σ, or both taken in concert, the scattering cross sections computed from Equation 12 must be insensitive to these changes. It has been demonstrated in this and in the companion paper (Harrison, 1968)[2] in various ways that this is true whenever $\sigma \gg \omega|\epsilon|$. But even if $k_1 a$ is markedly dependent on ϵ_r and σ, it is still possible for the scattering cross sections to be essentially constant in value. This is because of the complicated nature of Equations 3 and 4 and it would seem impossible for anyone to have a mental grasp of what might happen.

Referring to the curves it appears that when $|\epsilon_r| \gg 1$ the scattering cross sections are very insensitive to σ regardless of the value of σ. The spheres behave as though they were perfectly conducting. But when σ lies in the range $10^{-7} \leq \sigma \leq 10^0$ and $|\epsilon_r|$ is fairly small the curves for $\sigma_s/\pi a^2$ and $\sigma_f/\pi a^2$ spread out. For example, in this region a sphere might have a larger scattering cross section for $\epsilon_r = 7.0$ than for $\epsilon_r = 30$. Evidently a considerable amount of work remains to be done to obtain and interpret data relating to scattering from slightly lossy dielectric spheres and from over dense plasma spheres when the medium is only slightly lossy.

The determination of σ and ϵ_r by radar measurements on the simplest three dimensional object--the sphere--even when assumed to be homogeneous appears to be impossible. It is the opinion of the writers that radar observations on the plumes of missiles, ionized wakes of re-entry vehicles, and fireballs associated with nuclear explosions are of no value for obtaining an estimate of the physical size of the ionized volume or for deducing the values of the constitutive parameters of the scattering obstacle σ and ϵ_r.

ACKNOWLEDGMENT

The writers thank Beverly Pankuch of Dikewood Corporation for programming this problem for computation on the CDC-6600 computer at the U.S. Air Force Weapons Laboratory, Kirtland Air Force Base. Deyoe Stark typed the manuscript, and Roma Schramm prepared the figures. The text was proof read by Virginia Southerland and Fern Harrison.

REFERENCES

1. Wyatt, Philip J., "Electromagnetic Scattering by Finite Dense Plasmas," J. Appl. Phys., Vol. 36, No. 12, pp. 3875-3881 (1965).

2. Harrison, C. W., Jr., Scattering from Imperfectly Conducting Spheres, Theoretical Considerations, Sandia Corporation SC-R-68-1691 (1968). (A copy of this Sandia Corporation Technical Report may be obtained on request from the Technical Information Department.)

3. Siegert, A. J. F., Radar System Engineering, Radiation Laboratory Series, Chap. 3, Sec. 3.2, Eq. 4, p. 64, McGraw Hill Book Co., Inc. (1947).

4. Wyatt, Philip J., "Improved Surface-Wave Description for Scattering fron Overdense Plasmas," J. Appl. Phys., Vol. 37, No. 9, p. 3641 (1966).

5. Taylor, C. D., Harrison, C. W., Jr., and Aronson, E. A., "Resistive Receiving and Scattering Antenna," IEEE Trans. on Ant. and Prop., Vol. AP-15, No. 3, pp. 371-376, Figure 3 (1967). (See also the note by Cassedy et al in the January 1968 issue of the same journal relating to this subject.)

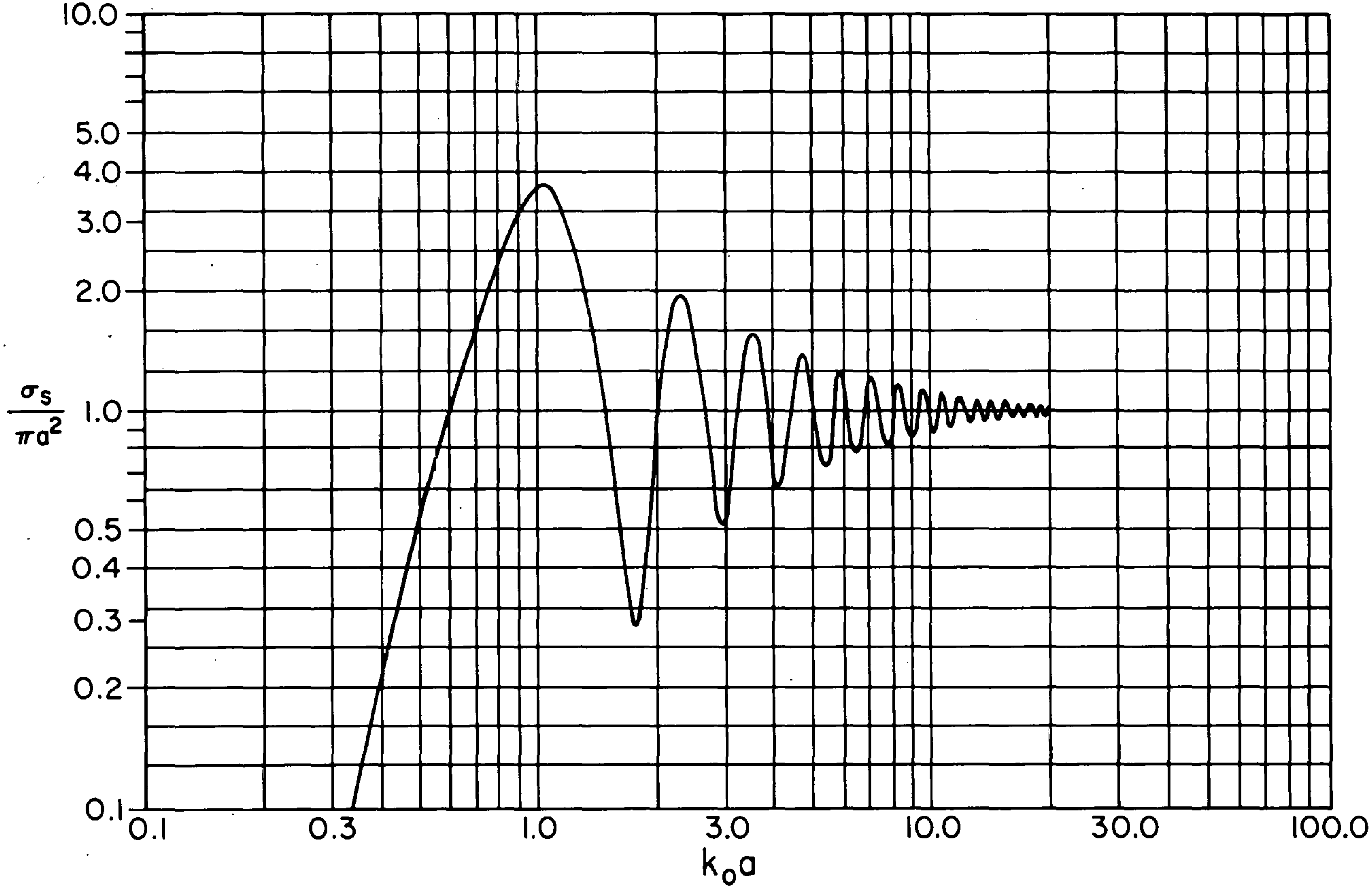

Figure 1. Backscattering Cross Section of a Perfectly Conducting Sphere

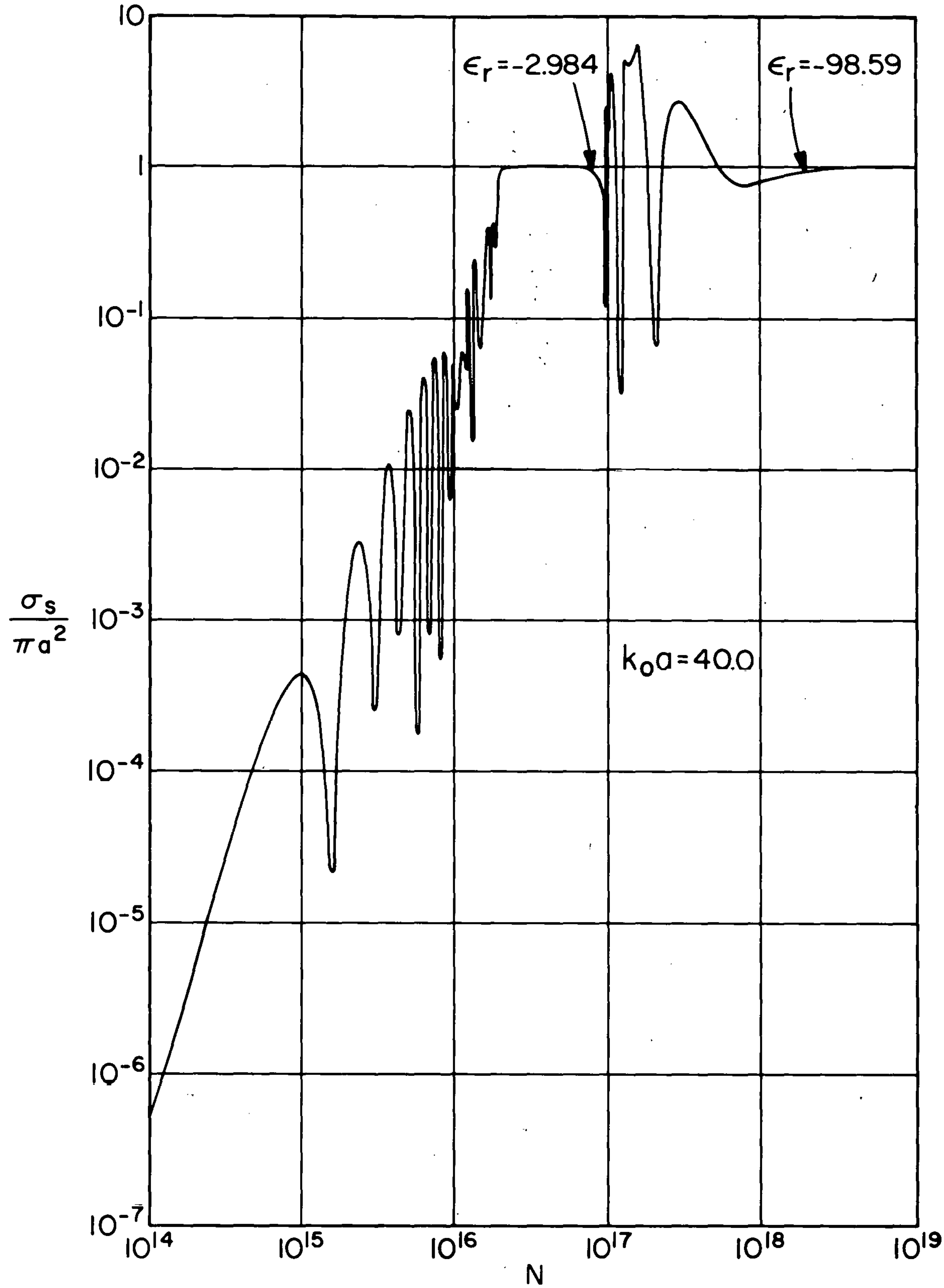

Figure 2. Backscattering Cross Section of a Collisionless Plasma

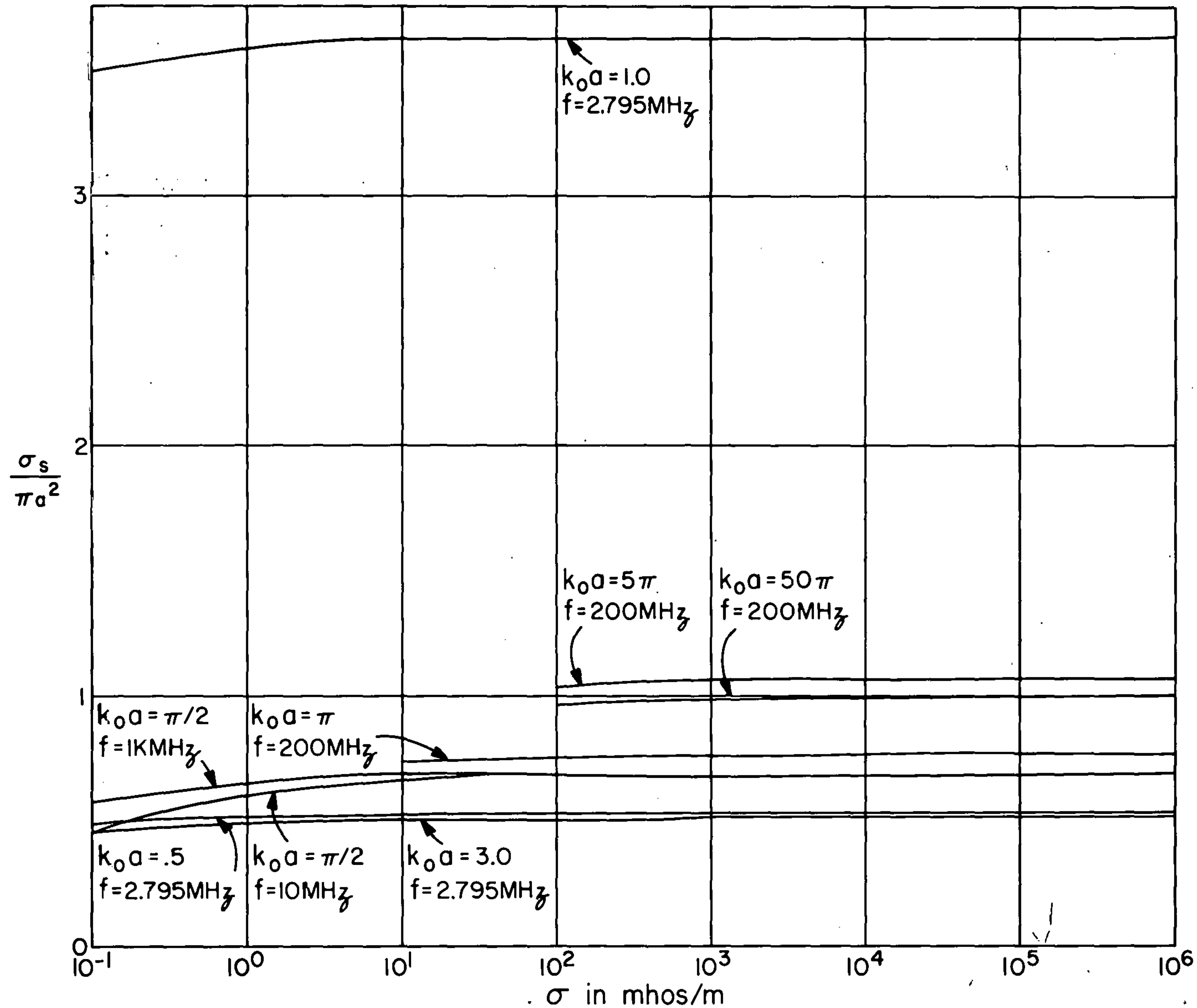

Figure 3. Backscattering Cross Section of a Sphere when $\sigma >> \omega|\epsilon|$

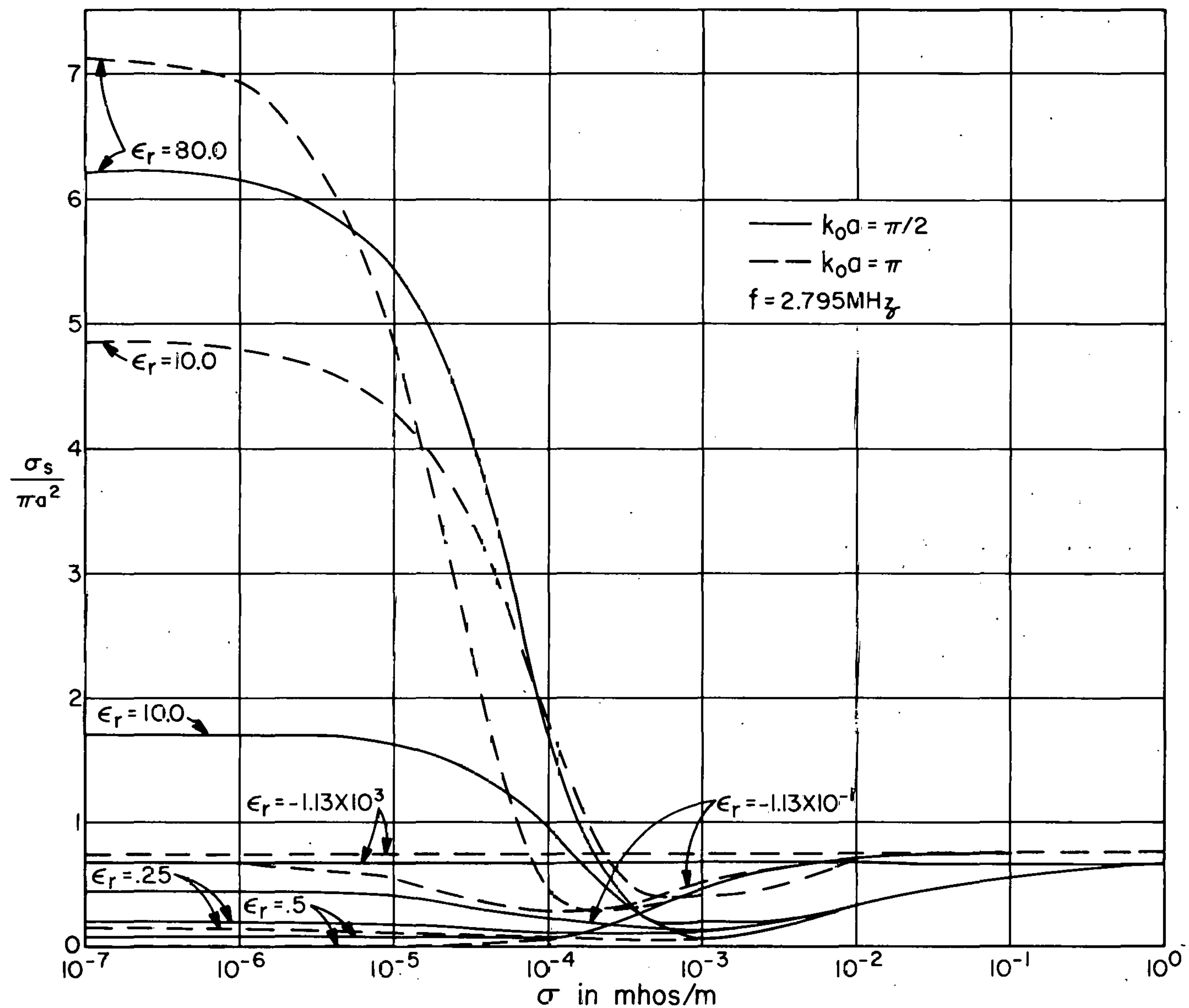

Figure 4. The Dependence of the Backscattering Cross Section of a Sphere on Conductivity for Fixed $k_o a$

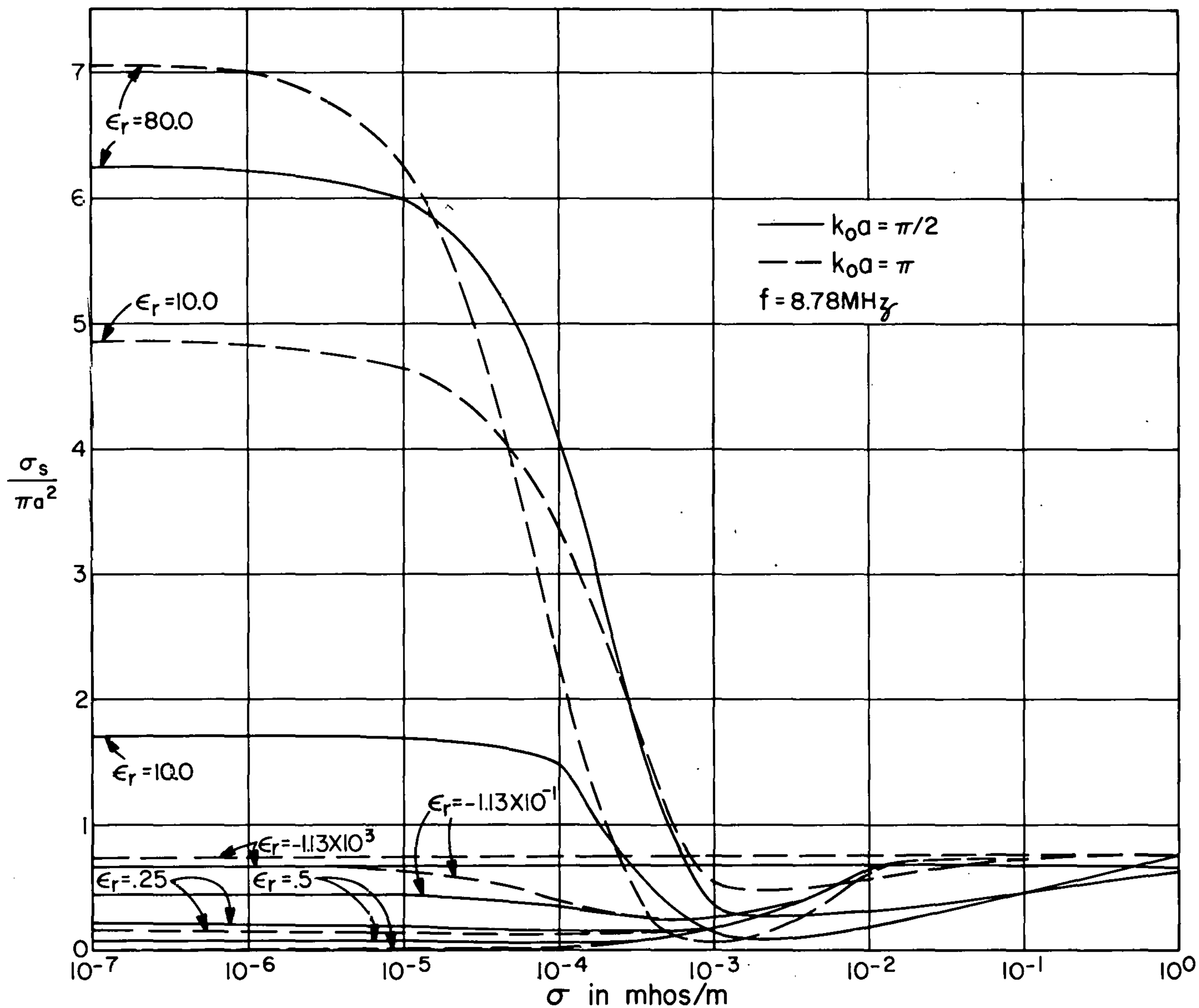

Figure 5. Like Figure 4, but for a Different Frequency

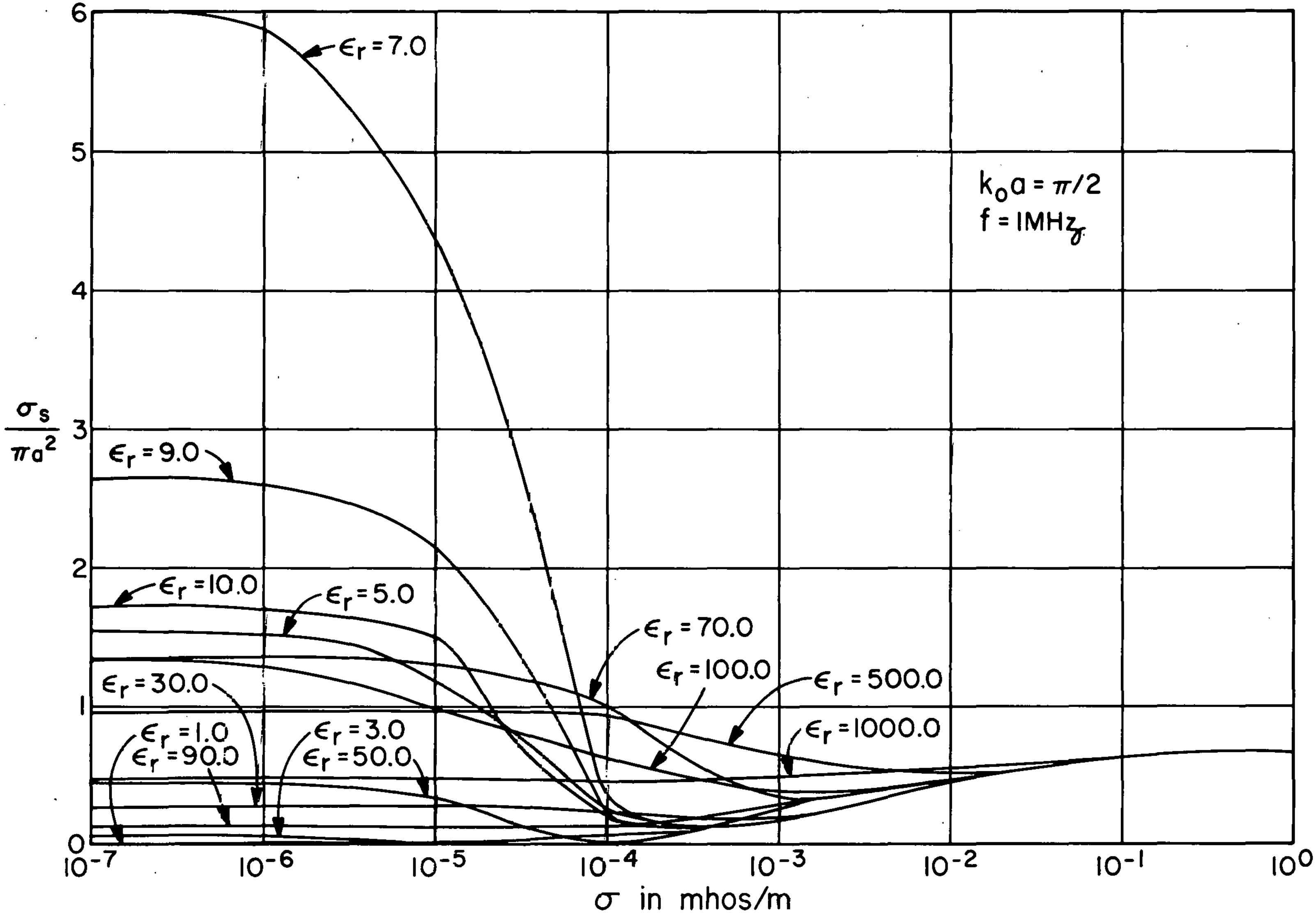

Figure 6. Like Figure 4, but for a Different Frequency

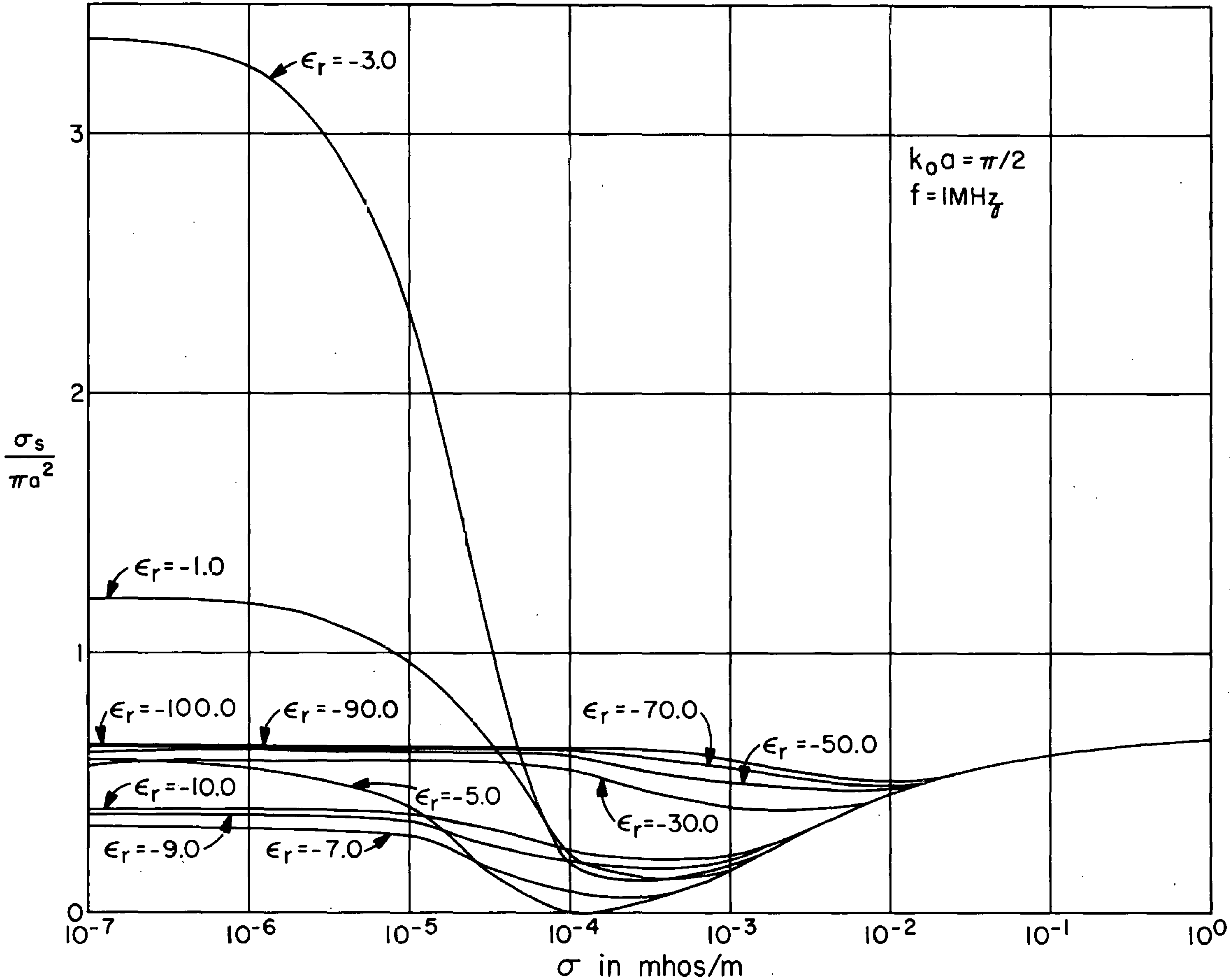

Figure 7. Like Figure 6, but for Negative Dielectric Constants

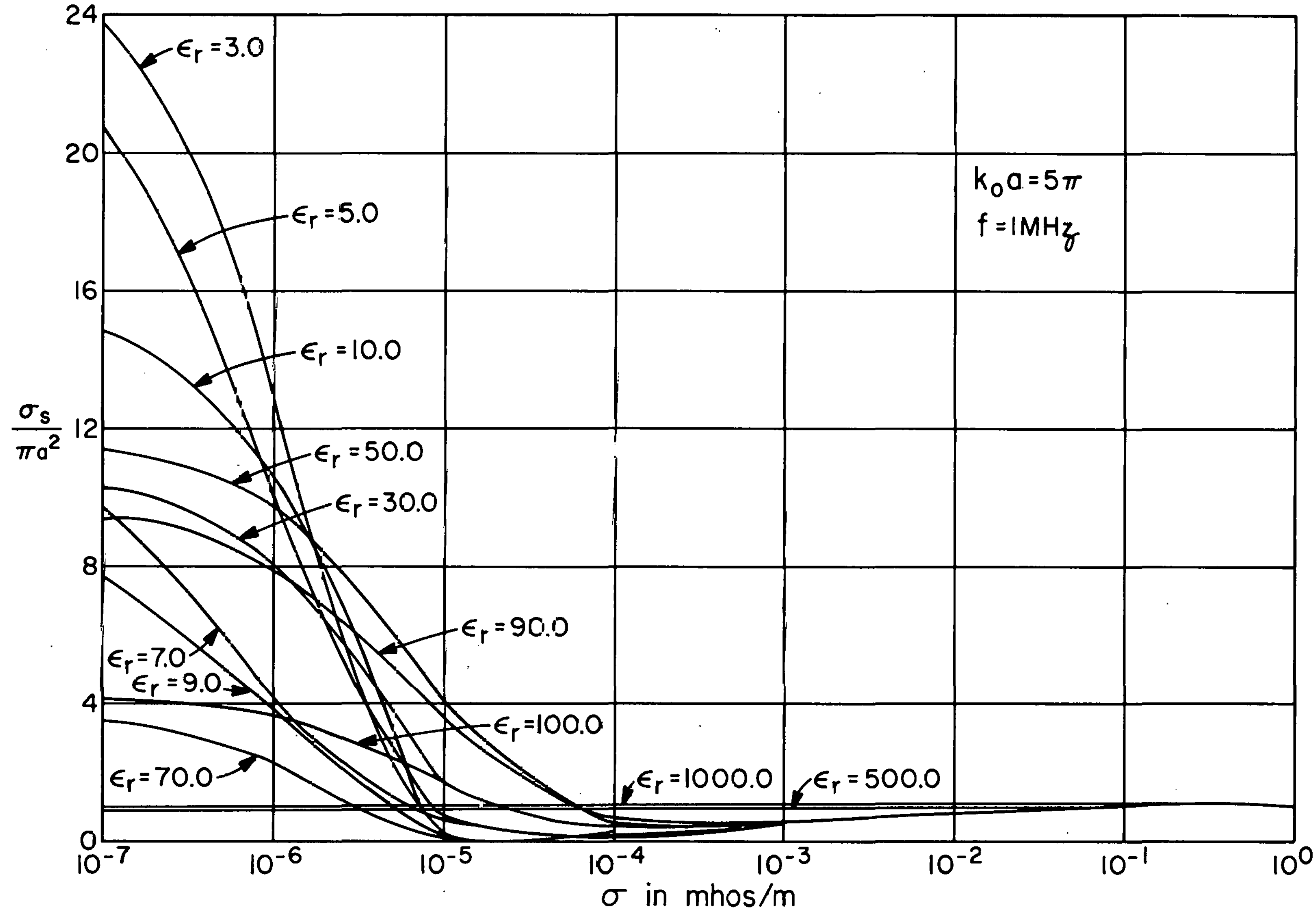

Figure 8. Like Figure 6, but for a Different $k_o a$

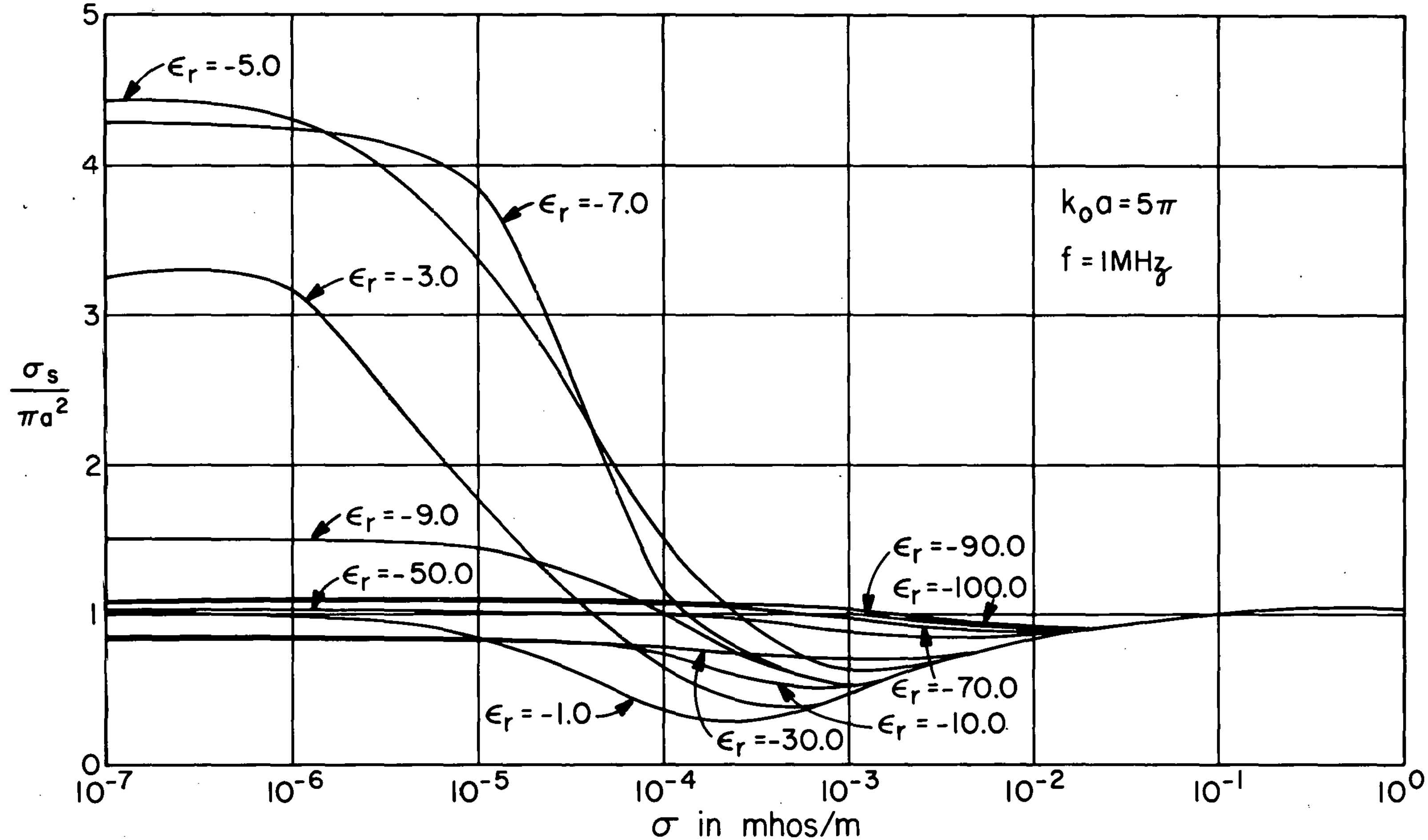

Figure 9. Like Figure 8, Except for Negative Dielectric Constants

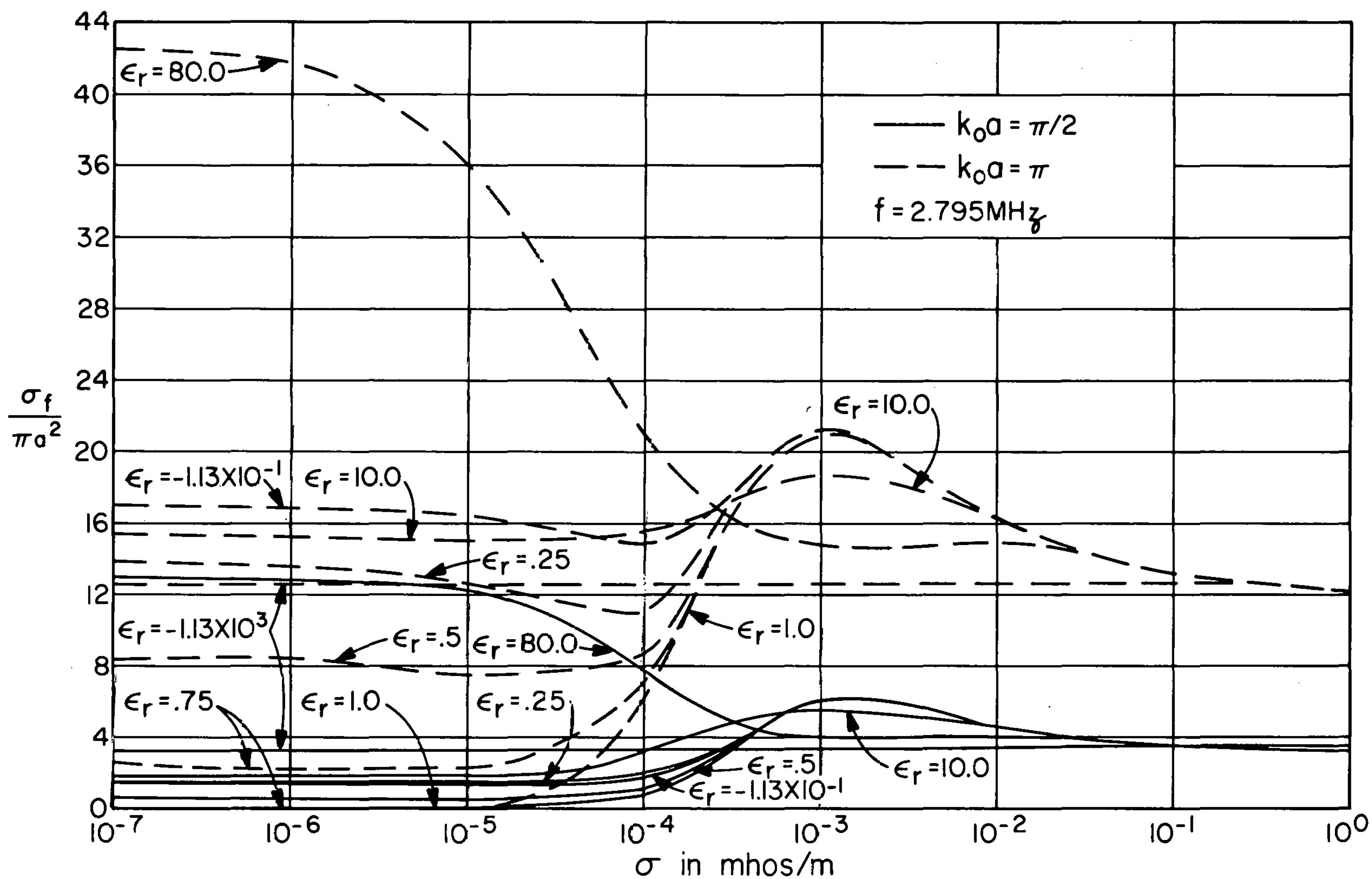

Figure 10. Like Figure 4, Except that Forward Scatter Cross-Section Data is Presented

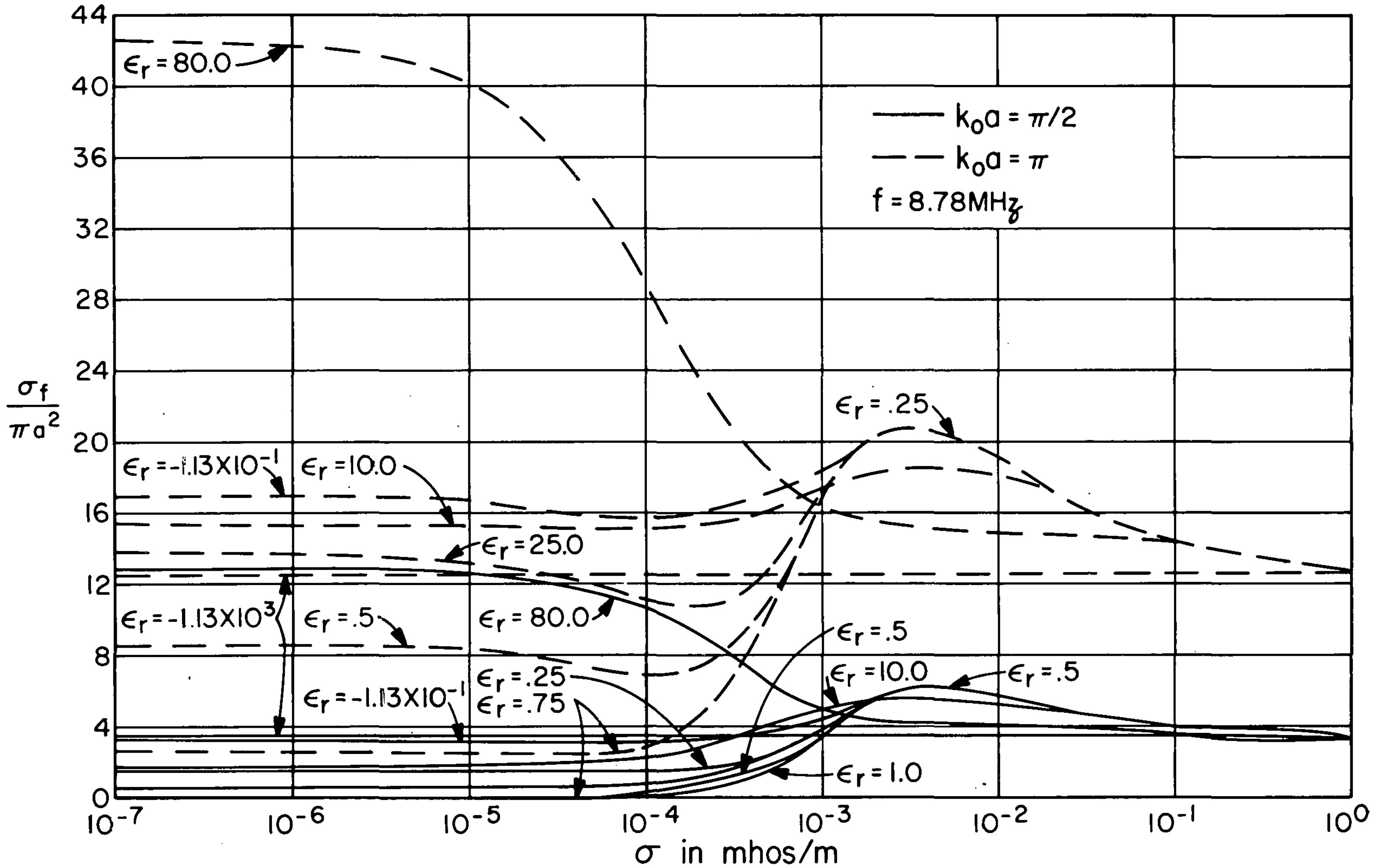

Figure 11. Like Figure 10, but for a Different Frequency

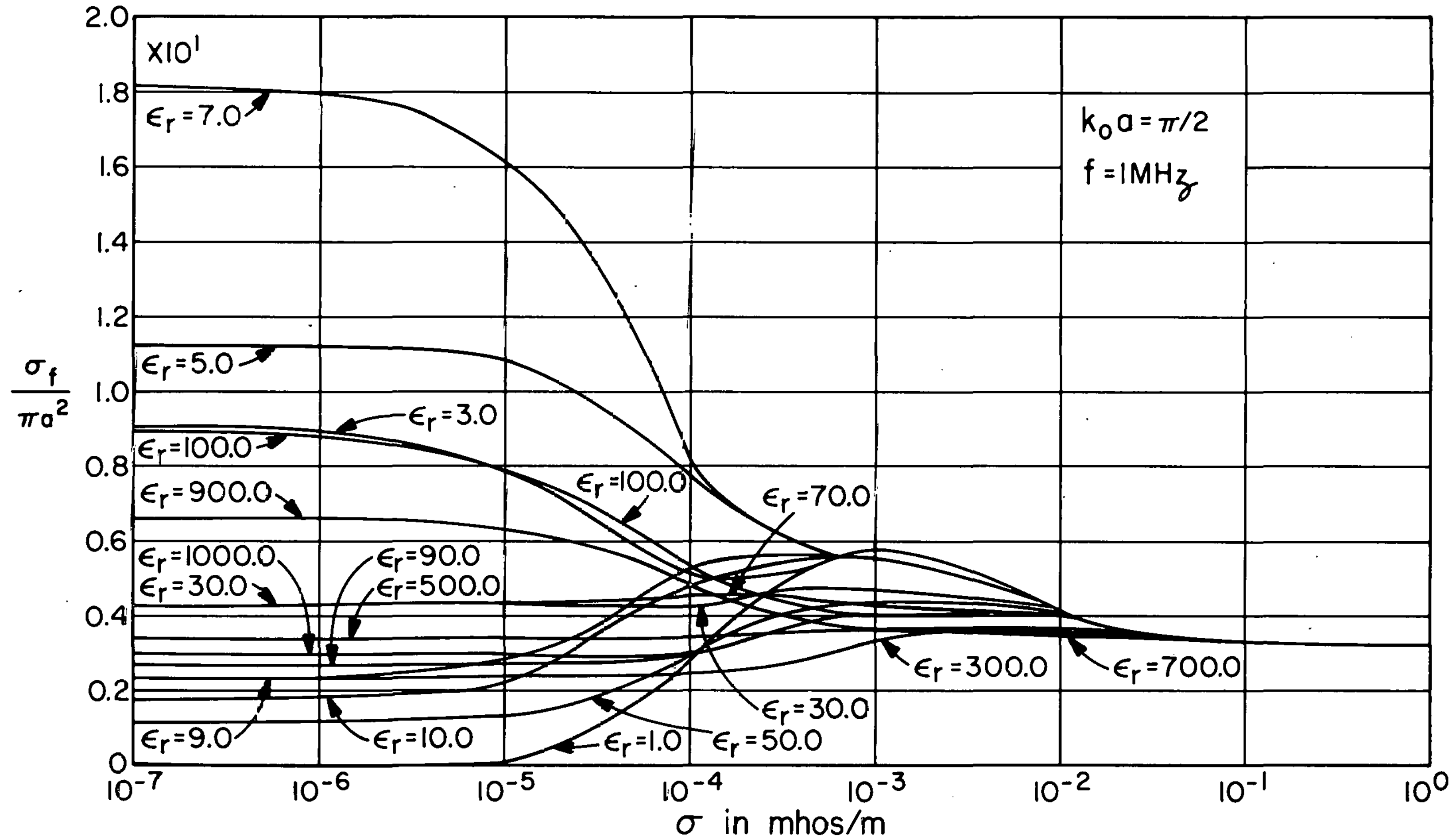

Figure 12. Like Figure 10, Except for a Different Frequency

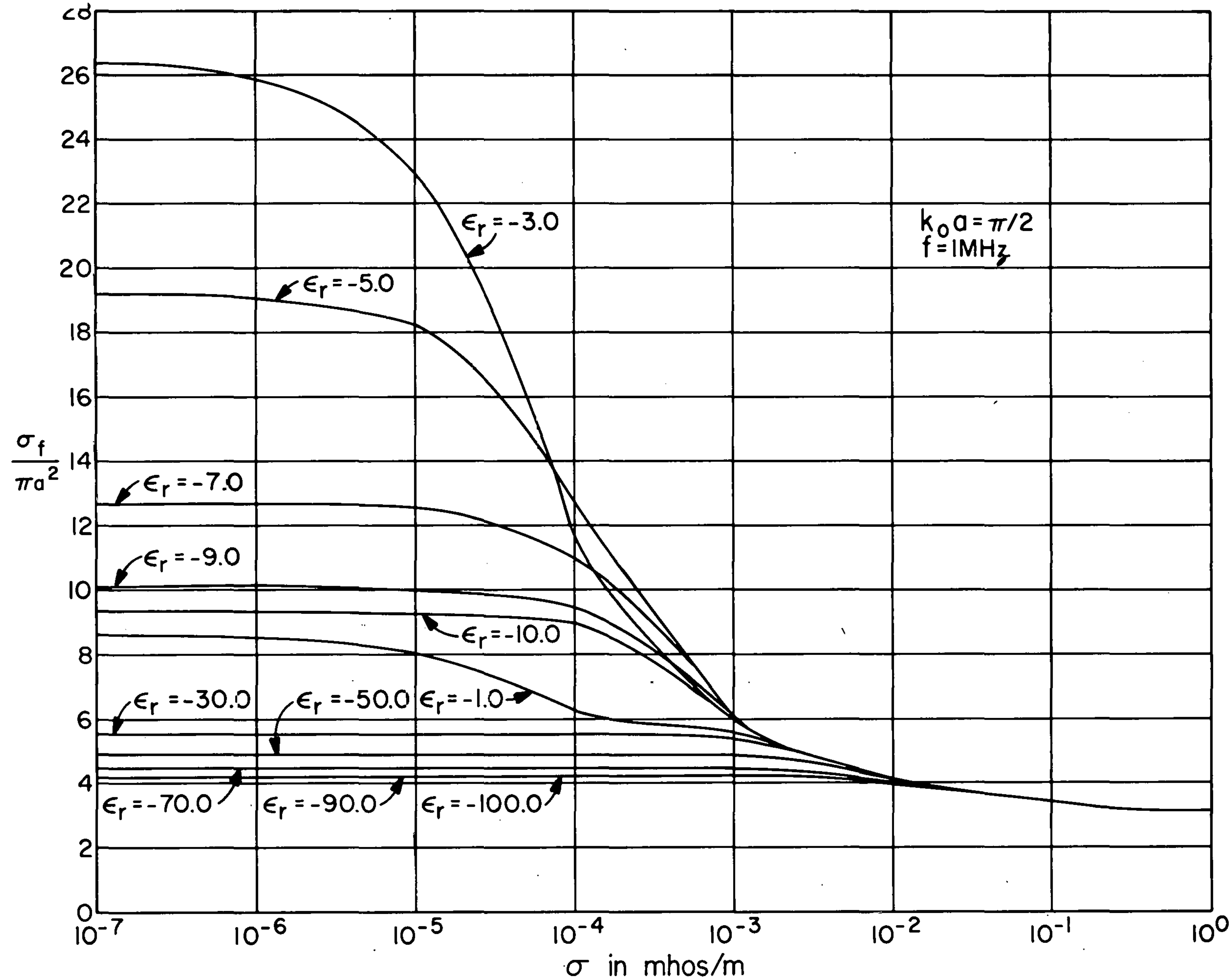

Figure 13. Like Figure 12, Except for Negative Dielectric Constants

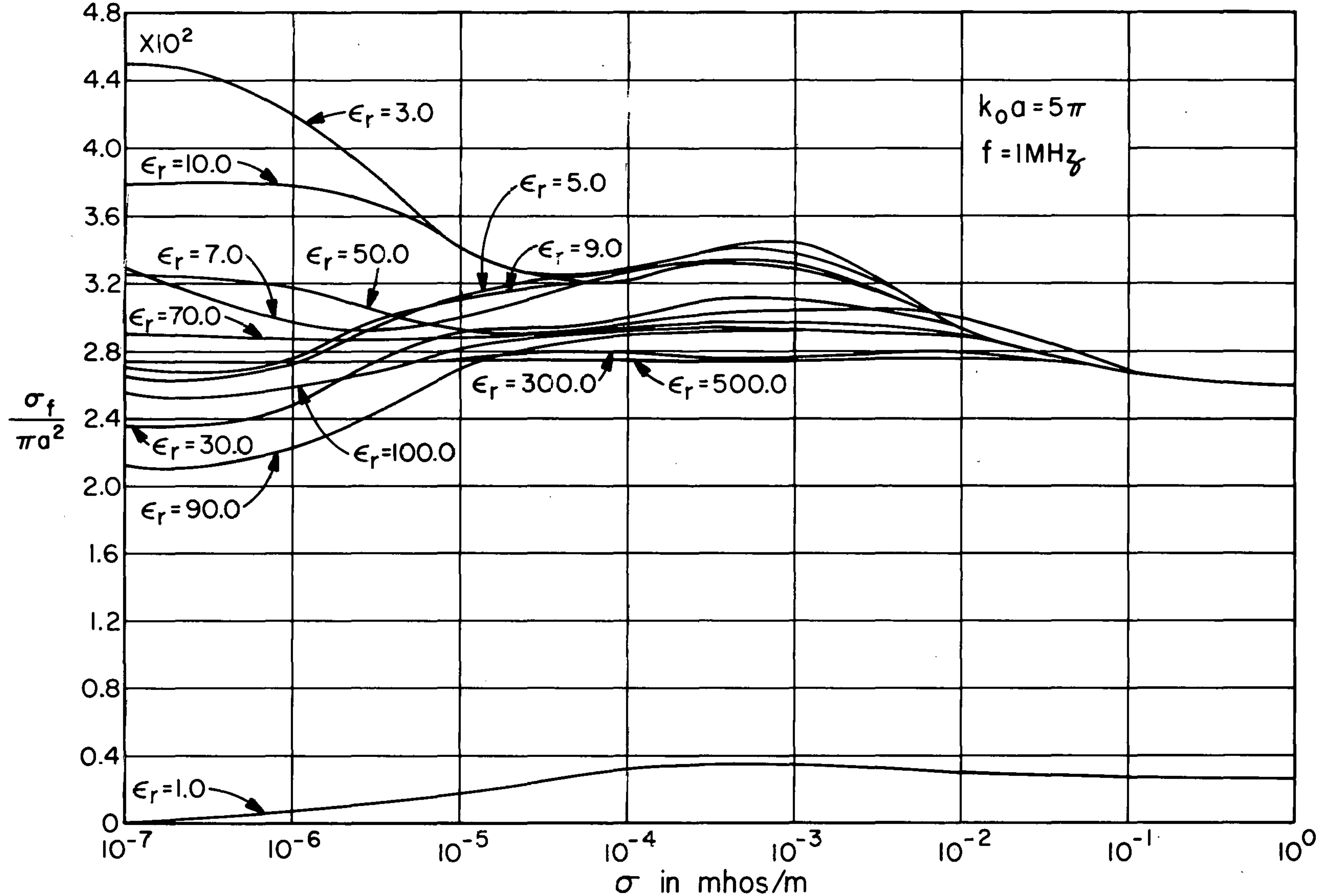

Figure 14. Like Figure 12, Except for a Different $k_o a$

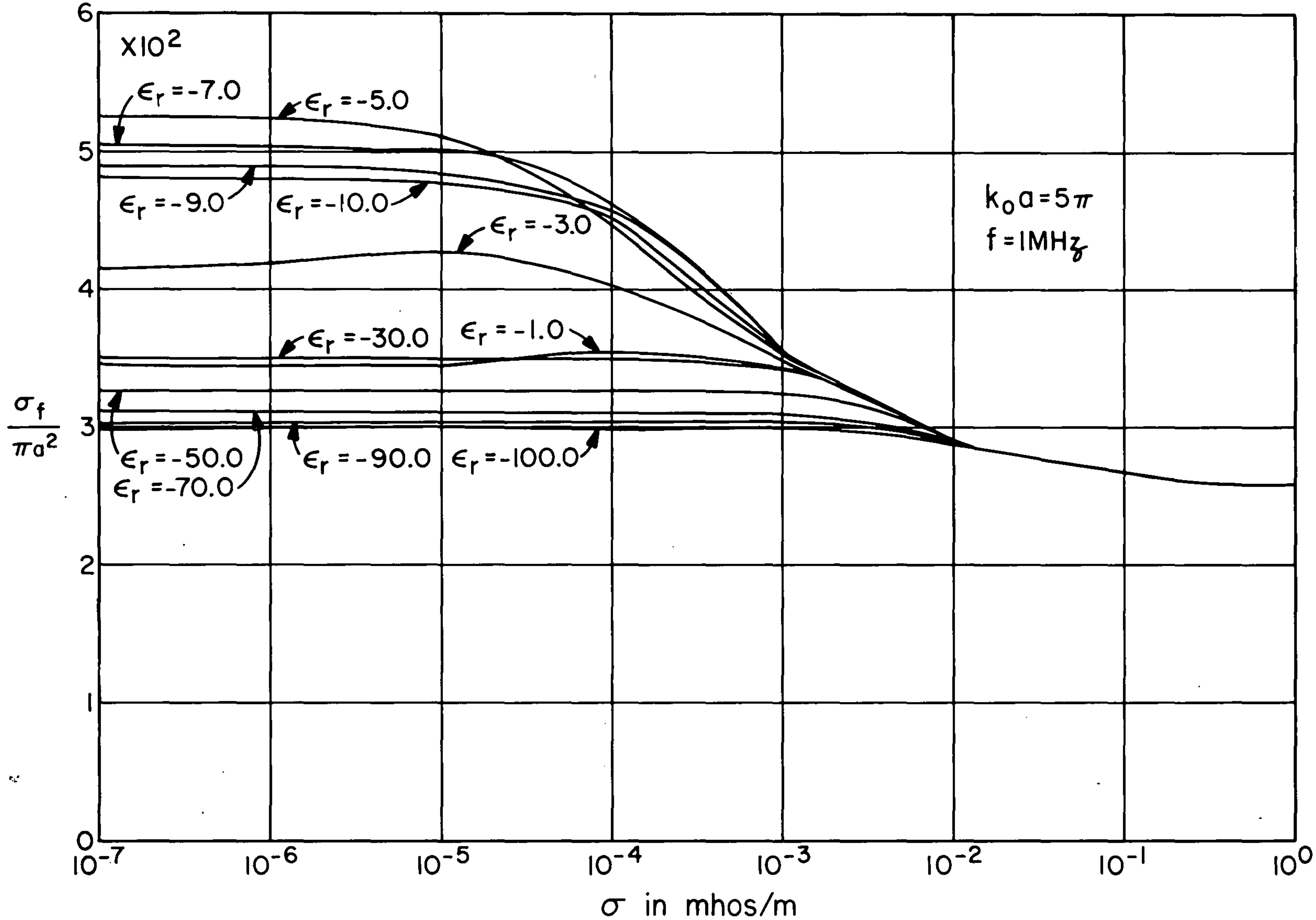

Figure 15. Like Figure 14, Except for Negative Dielectric Constants

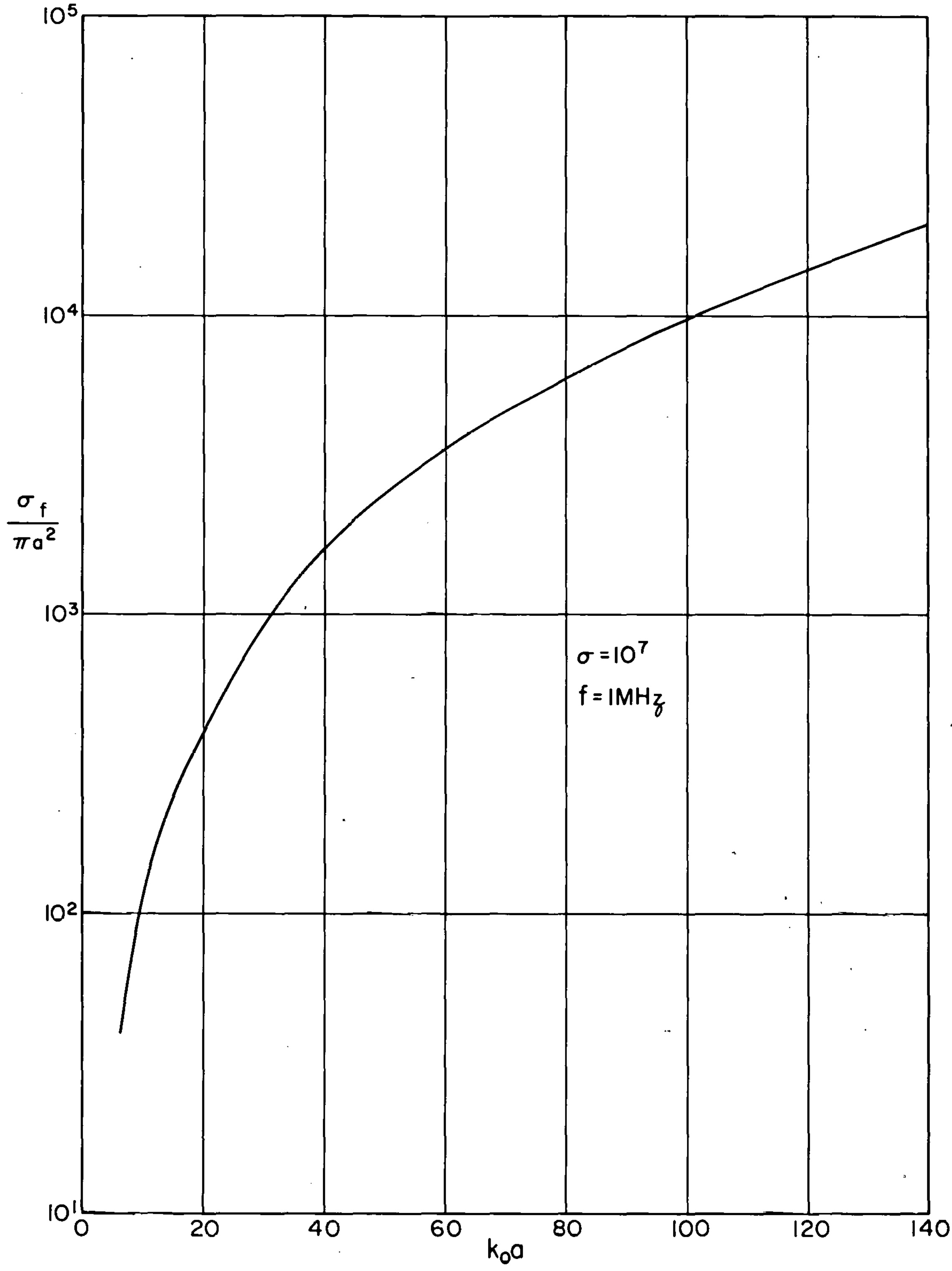

Figure 16. Forward Scattering Cross Section of a Highly Conducting Sphere

Figure 17. The Dependence of the Backscattering Cross Section of a Sphere on Relative Dielectric Constant for Fixed Conductivity

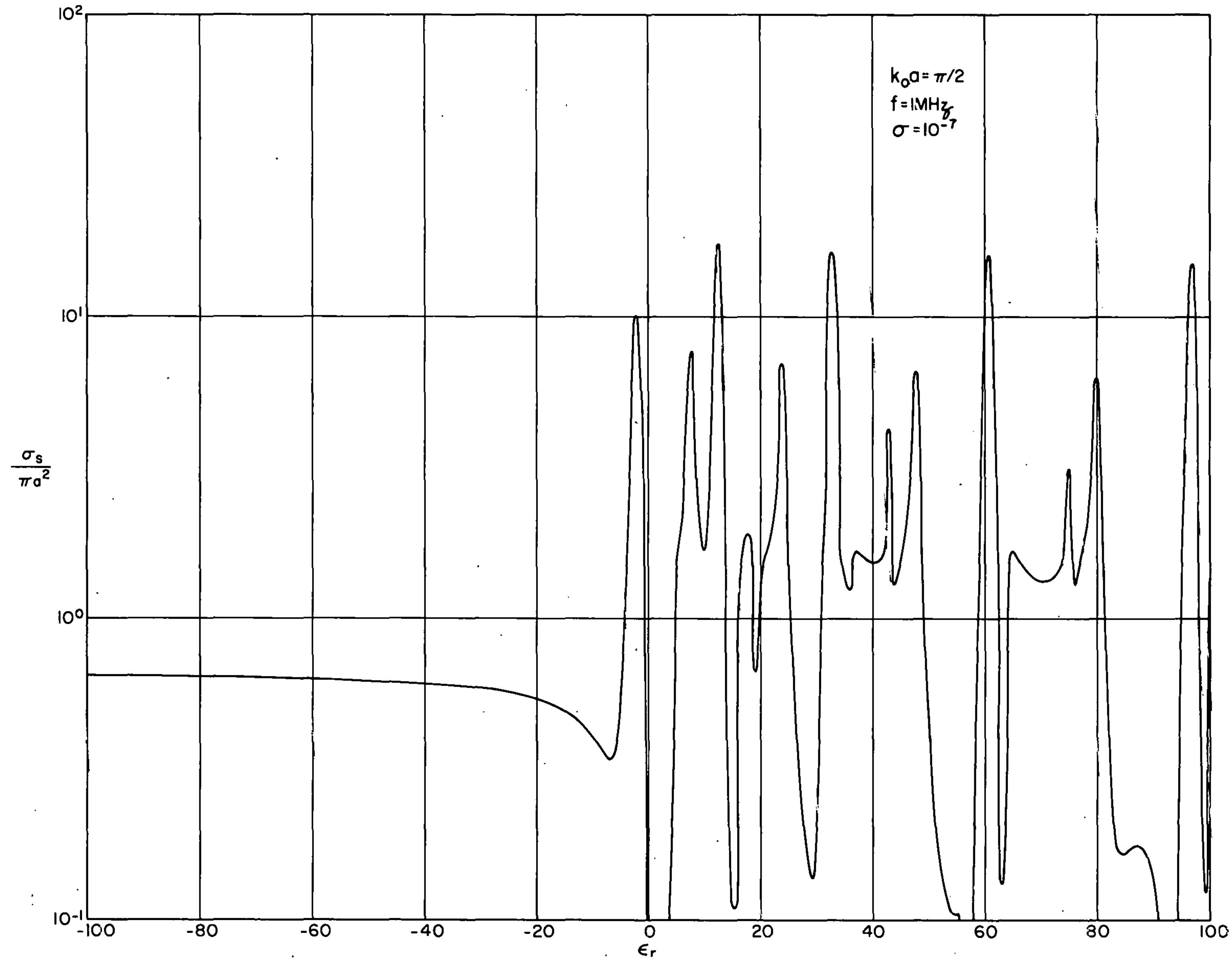

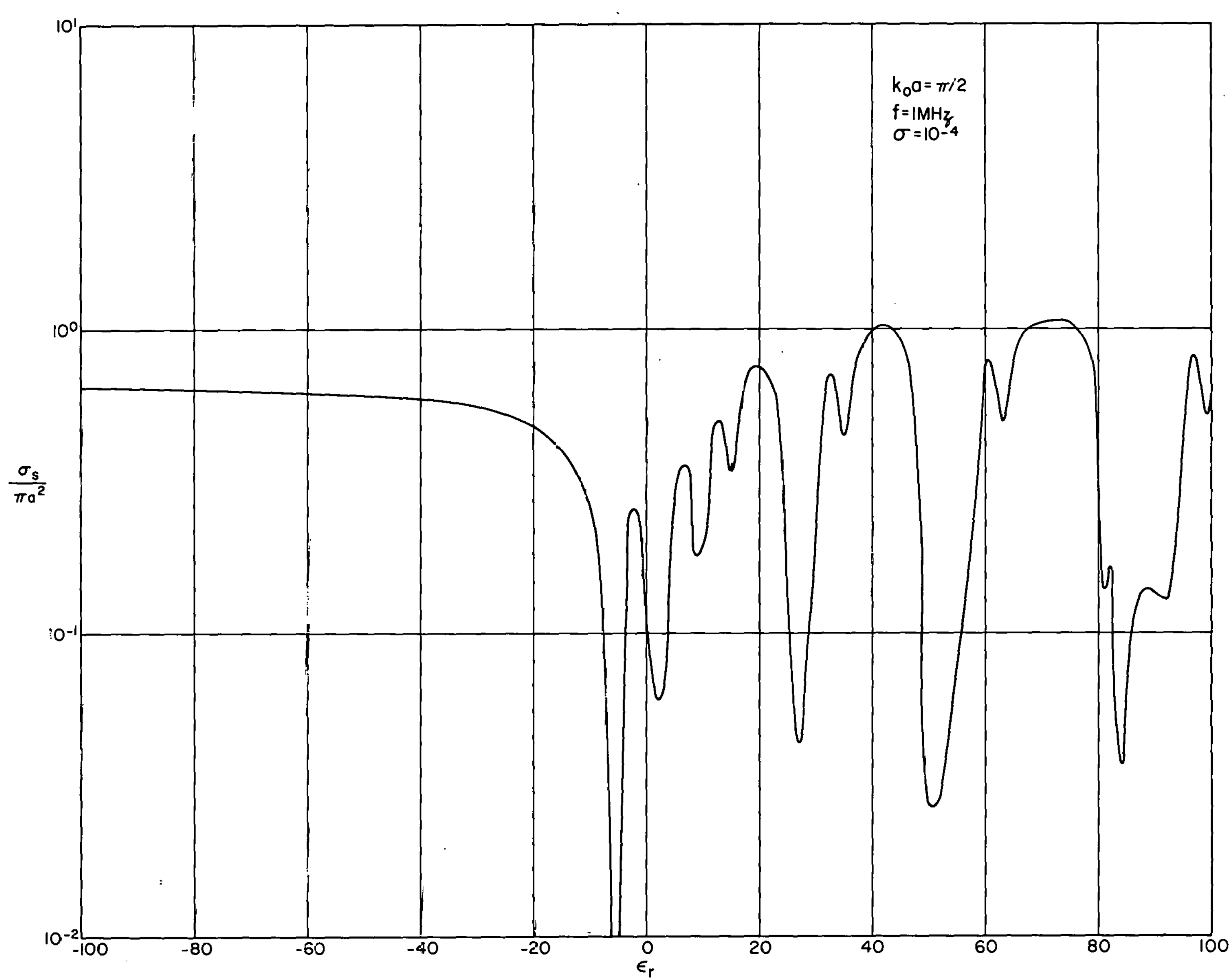

Figure 18. Like Figure 17, but for a Different Value of Conductivity

Figure 19. Like Figure 17, Except that Forward Scatter Cross-Section Data is Presented

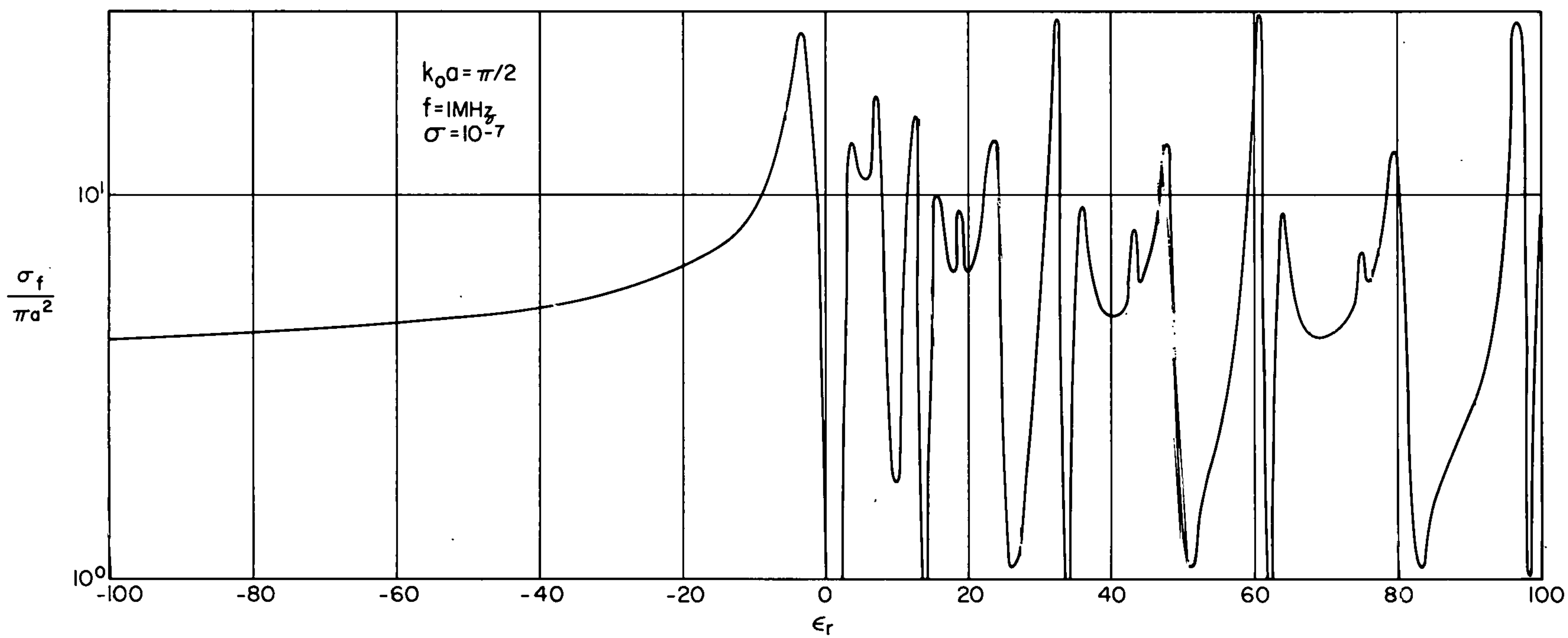

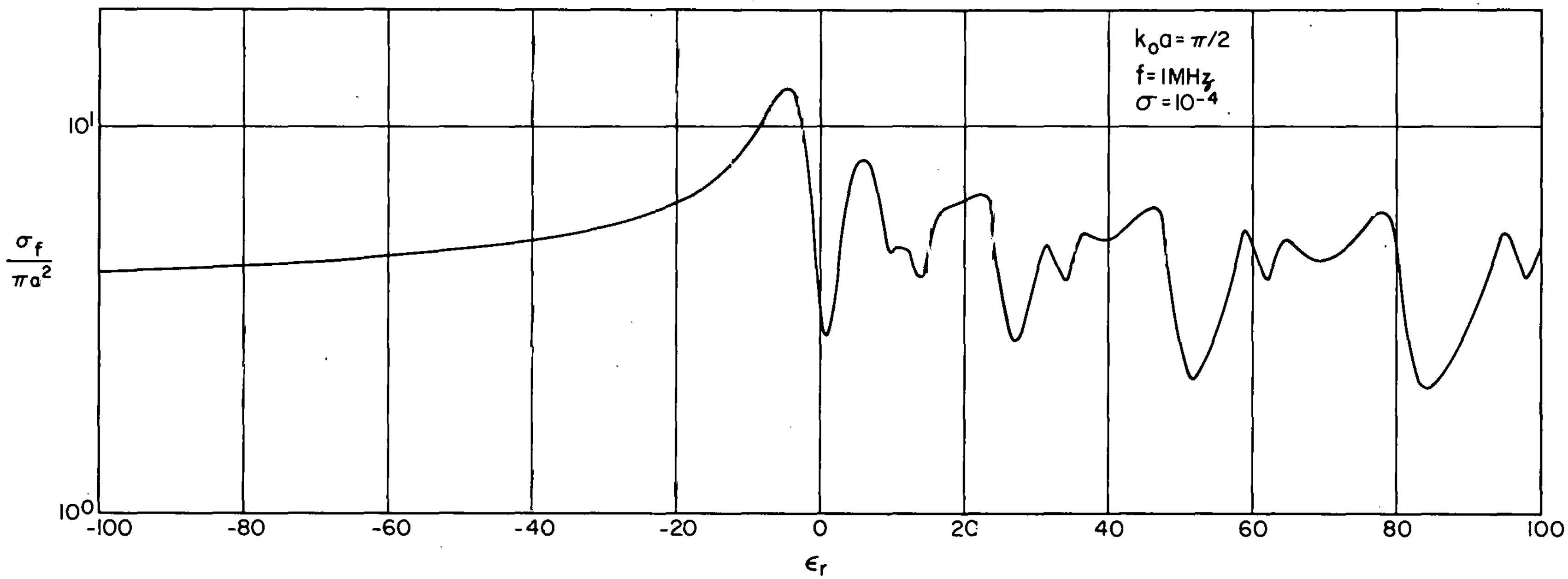

Figure 20. Like Figure 19, but for a Different Value of Conductivity